European Commission

JRC SCIENCE AND POLICY REPORTS

Space Weather Impact on the Scandinavian Interconnected Power Transmission System

Roberta Piccinelli and Elisabeth Krausmann

2015

Report EUR 27571 EN

European Commission
Joint Research Centre
Institute for the Protection and Security of the Citizen

Contact information
Elisabeth Krausmann
Address: Joint Research Centre, Via E. Fermi 2749, 21027 Ispra (VA), Italy
E-mail: elisabeth.krausmann@jrc.ec.europa.eu

https://ec.europa.eu/jrc

JRC98593

EUR 27571 EN

ISBN 978-92-79-53761-5

ISSN 1831-9424

doi:10.2788/939973

Luxembourg: Publications Office of the European Union, 2015

Abstract

Geomagnetic storms (GMS) can seriously affect high voltage power transmission grids. More specifically, GMS can inject geomagnetically induced currents (GICs) into the power network, thus causing instabilities and eventually leading to grid collapse. Since GMS are expected to cause more pronounced disturbances at high latitudes, this report addresses the effects of GMS on the Scandinavian interconnected power transmission grid, including Finland, Sweden and Norway. By applying 100-year-benchmark scenarios, we analyzed potential space-weather triggered voltage instabilities in the power grid considering mono-phase transformers, which are known to be more vulnerable to GIC injection, and three phase transformers, which are less vulnerable.
Our simulations indicate that the three-phase configuration of the network is significantly more robust than the mono-phase one. For a system with only three-phase transformers, the likelihood of grid collapse is very low, and collapse only occurs for the worst-case scenario with extremely high geoelectric field intensities. Our results indicate that lines that experience higher reactive power losses during normal operation are more likely to increase losses during a GMS event. According to our study, the portion of the Scandinavian interconnected power transmission grid most vulnerable to extreme space weather is the part where the highest reactive losses in transmission lines and in voltage magnitudes are observed. This corresponds to the southern parts of Sweden and Norway.
In the near future, this study will be extended to assess the risk of extreme space weather for larger portions of the EU power grid.

Space weather impact on the Scandinavian interconnected power transmission system

Roberta Piccinelli and Elisabeth Krausmann

Abstract

Geomagnetic storms (GMS) can seriously affect high voltage power transmission grids. More specifically, GMS can induce quasi-DC currents, known as geomagnetically induced currents (GICs), which enter the power network, thus causing instabilities and eventually leading to grid collapse. High-voltage power transformers are particularly susceptible to GIC impact: the injection of DC-currents drives transformers into their saturation regime, triggering undesired effects throughout the grid and, in case of intense currents, seriously damaging transformers.

Since GMS are expected to cause more pronounced disturbances at high latitudes, this report addresses the effects of GMS on the Scandinavian interconnected power transmission grid, including Finland, Sweden and Norway. By applying 100-year-benchmark scenarios, we analyzed potential space-weather triggered voltage instabilities in the power grid considering mono-phase transformers, which are known to be more vulnerable to GIC injection, and three phase transformers, which are less vulnerable.

Our analysis shows how the electric-field magnitudes and the power line orientation with respect to the geomagnetic field can inject currents of different intensities into the system and how their effect on the grid is susceptible to the power flow that drives GICs through the systems. GIC-induced instabilities in the system superimposed on the load flow increase the possibility for the system to collapse.

Our simulations indicate that the three-phase configuration of the network is significantly more robust than the mono-phase one. For a system with only three-phase transformers, the likelihood of grid collapse is very low, and collapse only occurs for the worst-case scenario with extremely high geoelectric field intensities. Our results indicate that lines that experience higher reactive power losses during normal operation are more likely to increase losses during a GMS event. According to our study, the portion of the Scandinavian interconnected power transmission grid most vulnerable to extreme space weather is the part where the highest reactive losses in transmission lines and in voltage magnitudes are observed. This corresponds to the southern parts of Sweden and Norway.

In the near future, this study will be extended to assess the risk of extreme space weather for larger portions of the EU power grid.

Table of Contents

1. Introduction

On 17 March 2015, the Space Weather Prediction Center (SWPC) of NOAA issued the following space weather advisory (NOAA, 2015):

```
Space Weather Message Code: ALTK08
Serial Number: 18
Issue Time: 2015 Mar 17 1401 UTC


ALERT: geomagnetic K-index of 8
Threshold Reached: 2015 Mar 17 1358 UTC
Synoptic Period: 1200 – 1500 UTC


Active Warning: Yes
NOAA Scale: G4 – Severe


Potential Impacts: Area of impact primarily poleward of 45 degree
Geomagnetic Latitude.

Induced Currents – Possible widespread voltage control problems and some
protective systems may mistakenly trip out key assets from the power
grid. Induced pipelines currents intensify […].
```

A severe geomagnetic storm (GMS) following a coronal mass ejection (CME) impact occurred which was classified at level G4 out of a scale of only five levels. Its impact on Earth caused an induced electric field of 200 mV/km, as calculated for New England power plant locations (NOAA, 2015). To give an idea of the intensity of the storm, the measured induced electric field was a tenth of the March 13, 1989 values, which caused a 9-hour blackout for the entire Québec region. This time, no power failures were reported.

The critical infrastructure that society has become most reliant on is the power grid. Power networks play a vital role in everyday life either as a standalone critical infrastructure providing electrical power but also as a service provider to many other critical infrastructures that critically rely on the power grid. In a report published by Kappenman (2010), it is claimed that a severe geomagnetic storm, like the Carrington event in 1859, could severely affect and damage the power grid, creating a dark era for our society. The question that arises is: are power transmission grids robust against geomagnetic storm impacts?

The aim of this work is to understand if power grids are stable and robust against space weather. In a previous report (Piccinelli and Krausmann, 2014) we addressed the problem by identifying the physical and technological part of the issue and introducing a complex network theory approach in order to understand the behavior of the power transmission grid. In this report, we apply our approach to the Scandinavian interconnected 400kV power transmission grid to understand the behavior of the network in case of extreme space weather events.

2. Model and failure modes

2.1 Geomagnetically induced currents (GICs)

This section briefly summarizes the physical phenomenon at the origin of the formation of GICs and reviews the most important factors that cause a power transmission grid to suffer from a GMS impact. The effects of geomagnetic storms on a power grid are shown in Figure 1.

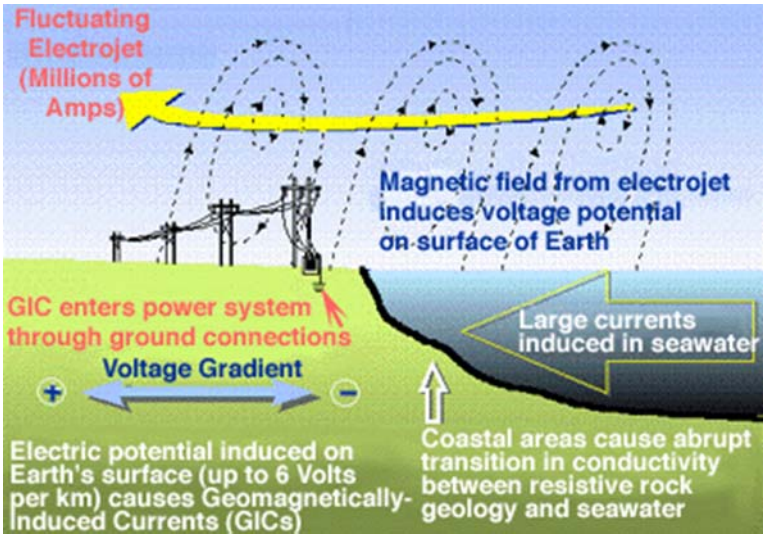

Figure 1. Schematic of the formation of geomagnetically induced currents (GICs) and of how they enter power grids (NOAA, 2015).

Geomagnetic storms appear on Earth as electrojets. These are flows of particles, which fluctuate in the ionosphere. They cause a time variation of the terrestrial magnetic field, which induces a voltage potential on the surface of the Earth. When such a potential “encounters” a closed circuit, it induces currents to flow in it. Power transmission grids are networks of long transmission lines and stations linked to the ground through grounded connections. Together with the ground, transmission lines form closed loops which, when being exposed to an electric potential, experience the induction of currents. This is the application of the well-known Faraday law: a time-varying magnetic field induces a current to flow in a closed loop.

When a geomagnetic storm hits the Earth, geomagnetically induced currents are formed and can enter the power transmission grids. The degree to which the geomagnetic storm affects the power system and its equipment depends on several factors. These include (NERC, 2012):

- Magnitude and orientation of the magnetic field
- Geomagnetic latitude
- Geology of the local area, including the electrical conductivity of the soil
- Proximity to an ocean or large water bodies
- Directional orientation, resistance and length of transmission lines
- Design of the power system and its equipment

We can separate these factors into two main classes: geo-physical factors, which are the first four points, and technical factors.

The site where the grounded stations are located and their geomagnetic characteristics are extremely important. Since the geomagnetic field deviates the particles coming from the Sun towards the poles, northern latitudes will be more affected by the electrojets. Moreover, since the ground acts as a conductor, the electrical conductivity of the soil determines how much current will enter the station: a conductive soil will limit the quantity of current entering the power grid; in contrast, a less conductive ground will allow more induced current to enter the system. The presence of an ocean or of a large body of water can also influence the ground conductivity, increasing the quantity of currents entering the system.

The technical factors that concern the engineered system are its structure, in terms of orientation and electrical characteristics of the transmission lines, and the characteristics of its components.

GMSs can affect the components and the operation of power systems through a wide range of impacts. Effects with minor severity may be the tripping of electrical equipment or control malfunctions. Major GMSs may trigger voltage and reactive power fluctuations, local disruption of service, equipment failure and potential voltage instability that can potentially result in the uncontrolled cascading of the bulk power system.

2.2 Transformers

Transformers are among the power grid components that are most susceptible to GIC impact. They are also among the most important components of the grid: since their function is to allow the transformation of a precise quantity of voltage, each transformer is specifically designed for a certain location of the system. The procedure of designing, producing, transporting and installing a transformer is costly and time-consuming and may require from twelve up to eighteen months. It is not feasible to keep in stock too many reserve transformers, so it is of the utmost importance for the stakeholders and operators to protect transformers from damage due to GICs.

GICs are quasi-DC currents that can cause numerous problems when entering the power grid. Transformers are particularly susceptible to GIC impact, as they are not designed to handle the DC current. In fact, almost all power grid equipment and operational problems due to space weather arise from disturbed transformer performance, which is driven into half-cycle saturation by the GIC. As a consequence, the normally nearly linear relationship between input and output voltages and currents is shifted into a non-linear region. A number of secondary effects follow, such as increased reactive power consumption and the injection of even and odd harmonics into the power system. These harmonics cause even less compensating reactive power to be available, which can eventually lead to grid collapse (Molinski, 2002). Boteler (2001) notes that the situation is worse for power grids with long transmission lines, e.g. in the range of hundreds of kilometers, because longer lines have higher voltage support requirements.

The following sections briefly describe the main damage and failure modes associated with GIC loading in power grids.

Transformer saturation

Power transformers are used for stepping up voltage levels for electricity transport in transmission lines or reducing the voltage for electricity distribution to the customers. They use steel cores and are designed to be extremely efficient. As shown in Figure 2 (left), transformers usually operate in the linear range of their magnetic characteristic, which corresponds to an exciting current of only a few Amperes of AC. If GICs flow in the system, the operating point on the steel core saturation curve is shifted towards the nonlinear portion of the characteristic (Figure2 right). Consequently, saturation occurs during one half of the cycle, causing a very high and asymmetrical exciting current (10-15% or more of the rated load current) to be drawn by the transformer (Ngnegueu et al, 2012).

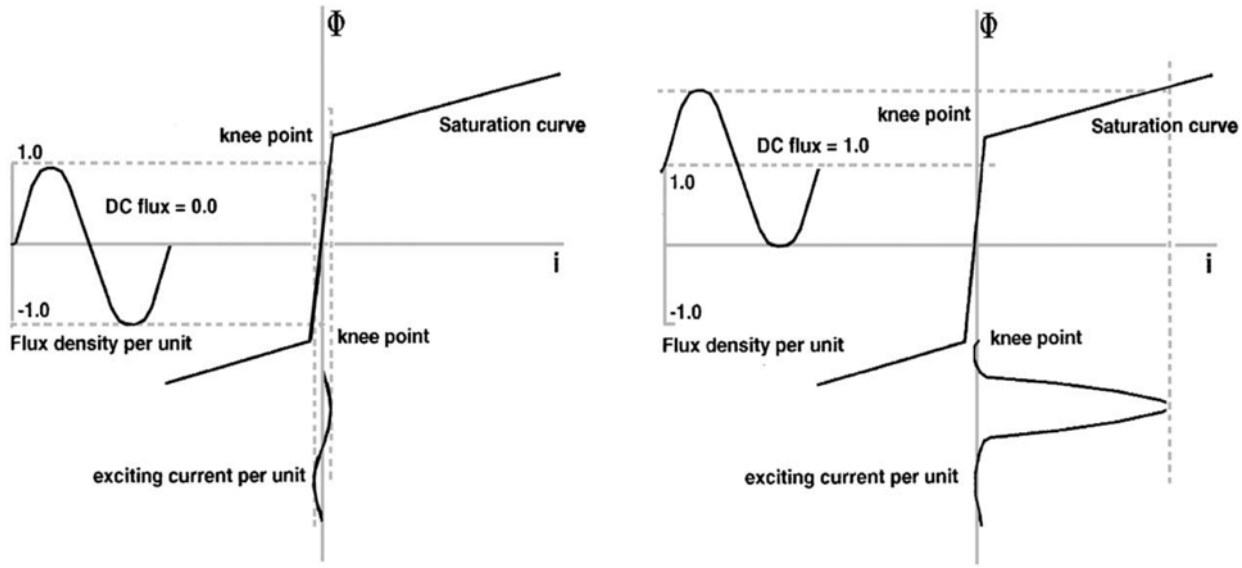

Figure 2. Relationship of exciting current and magnetic flux under normal operating conditions (left) and in the presence of GICs (right) (Molinski, 2002).

Different transformer types are impacted differently by half-cycle saturation (Kappenman, 2010). Single-phase transformers, in particular, are more at risk than three-phase transformers because the quasi DC flux induced by the GIC can flow directly in the core. Furthermore, shell-type transformers are at greater risk than core-type transformers while autotransformers are particularly susceptible (Kappenman, 2010).

Reactive power losses

Transformers saturated by GIC loading have a higher reactive power consumption, which increases linearly with GIC magnitude (Albertson, 1973; Walling and Kahn, 1991). Single-phase transformers consume the largest amount of reactive power. A 90° voltage shift caused by the excitation current during saturation creates a reactive power demand from the power system. As a consequence, there may be drops in system voltage and the stability margins may decrease significantly because additional reactive power is being consumed. The situation is exacerbated if voltage support devices trip during GIC events (Molinski, 2002) due to the injection of harmonics into the system.

Harmonics

When a transformer is driven into half-cycle saturation, the exciting currents contain harmonics of various orders (fundamental, 2^{nd}, 3^{rd}, etc.), giving rise to complex current patterns. In case of very large GIC levels, the contribution of harmonics declines, especially at the higher orders, since the transformer is operating in a completely linear, although saturated, region of its magnetizing curve (Molinski, 2002). Power grids are generally designed to cope with odd harmonics (e.g. 3^{rd}). However, they can be overwhelmed by even harmonics (e.g. negative sequence 2^{nd} harmonic) because they are usually not expected during power operations (Molinski, 2002). False neutral overcurrent relay actuation may be the consequence. Moreover, harmonic currents can also cause additional series losses in e.g. circuit breakers and filter banks.

Transformer overheating

In case of transformer saturation most of the excess magnetic flux flows externally to the core into the transformer tank, where currents are created and localized tank wall heating with temperatures reaching 175°C can occur (Kappenman, 1996). If a transformer is repeatedly exposed to heating due

to GIC loading, it can lead to cumulative insulation damage, accelerated ageing and eventually transformer failure (Koen and Gaunt, 2003). Unfortunately, in such cases it is usually not straightforward to relate cause and effect, so the real cause of transformer failure could be attributed to other reasons.

Generator overheating

Although no serious generator damage due to GMSs has been documented so far, there is at least theoretically some potential for damage (Molinski, 2002). Generators are usually shielded from direct GIC impact but they can still be affected by harmonics and voltage unbalance caused by transformer saturation. If harmonic currents enter the generator, excessive heating and mechanical vibrations can result. Moreover, the energy of the higher harmonic orders is concentrated near the rotor surface, which can also heat up and create a crack initiation site. As is the case for transformer heating, these phenomena may diminish the useful life of a generator, although the damage might not be immediately apparent and a potential failure at a later stage not necessarily attributed to GIC impact.

Protection relay tripping

In case of GIC flows, the harmonic content of the power system increases. With modern digital relays measuring the peak current value to monitor the status of the system, they are sensitive to tripping by harmonics. These false trips can then indirectly trigger a cascading failure of the power system. The relays' set current can be adjusted to accommodate the higher harmonics during GID impact and reduce the risk of false trips. However, this comes at the cost of lower protection levels (FEN, 2013).

Power systems increasingly depend on reactive power compensators and shunt capacitor banks for voltage control. Generally, shunt capacitors are grounded and have protection against unbalanced operation via neutral overcurrent relays. However, these capacitors banks are vulnerable to false trips during GMSs because of the capacitor's low impedance at the associated harmonic frequencies. Several power grid operators have upgraded or even replaced their neutral overcurrent unbalance protection to reduce the likelihood of false trips (IEEE, 1993).

The three primary effects of GICs on transformers and hence on power systems and their consequences is outlined in Figure 3.

The aim of this report is the study of the behavior of the power grid affected by a GMS: we are looking at the system as a whole so we focus our attention on the increase of reactive losses as the primary cause of collapse for the grid.

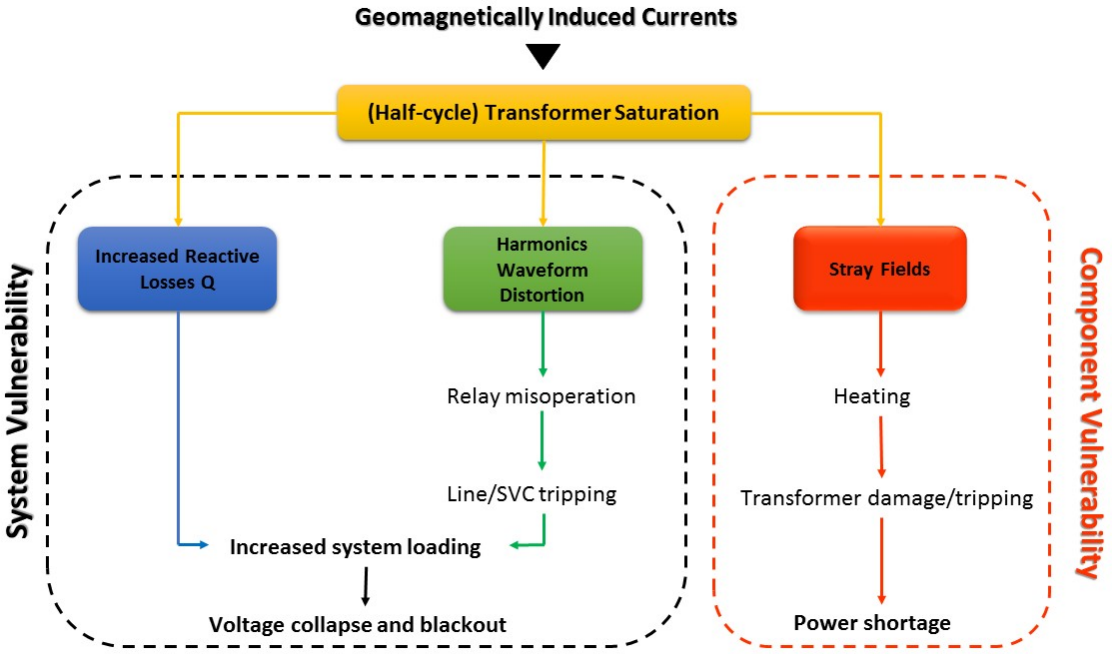

Figure 3. Overview of power system impact of GIC representing the effects of half-cycle saturation and their consequences.

3. Effects of geomagnetic storms on the Scandinavian interconnected power grid

In this section, we discuss the effects of GMS on power grids that connect Finland, Sweden and Norway. We will refine the benchmark model of the grid, which is a 17 node-Finnish grid, expand it and extend the analysis to cover also the Swedish and Norwegian 400 kV power transmission network.

3.1 GMS scenarios

Satellites providing timely space weather information and a network of magnetic observatories and distributed magnetometers monitoring Earth's magnetic field data in real time provide early indications of initiating solar storm events. Warnings can be received as short as 30 minutes before the beginning of impending geomagnetic storms. Nevertheless, no mathematical model is able to predict when a GMS will take place during a solar cycle and how intense it will be. In order to assess system performance during a low probability, high magnitude GMS event, a benchmark geomagnetic disturbance event was proposed by Pulkkinen et al. (2012). The model was completed using 10-second sampling of geomagnetic data covering more than one solar cycle and has the following characteristics:

- Earth's conductivity influences the electric field on the surface of the Earth, so we need to take it into account when calculating the electric field and resulting GICs. The benchmark model considers two earth conductivity scenarios, which represent two realistic extremes of a scale representing all possible type of soils: a conductive and a resistive ground structure;

- The scenarios also account for the different latitudes at which GMS have different intensity: the highest peaks are recorded at northern latitudes (above 60 degree of geomagnetic latitude), corresponding to the Scandinavian region, while smaller intensities are recorded at lower latitudes, corresponding to continental Europe.

The resulting four scenarios are summarized in Table I:

Scenario A |**E**|=20 V/Km High Latitude Low Conductivity	Scenario B |**E**|=5 V/Km High Latitude High Conductivity
Scenario C |**E**|=2 V/Km Low Latitude Low Conductivity	Scenario D |**E**|=0.5 V/Km Low Latitude High Conductivity

Table I. Schematic representation of the characteristics of the geoelectric field |E| for 100-year extreme GMS scenarios, as proposed by Pulkkinen et al. (2012).

The largest GIC measured in the Finnish 400 KV power system is as high as 201 A (on March 24, 1991) (Pirjola et al. 2003, 2005). Probably the largest measured GIC ever reported is 320 A in the Swedish power grid during the geomagnetic storm in April 2000 (Erinmez et al., 2002). Observations show that although rare, GICs amplitudes of several hundreds of amperes and geoelectric field magnitudes of the order of 10 V/km are possible (Pulkkinen et al., 2008).

In the study of the Scandinavian interconnected power transmission grid we considered Scenarios A and B which are the scenarios above the threshold geomagnetic latitude for the countries included in the study. Scenario A represents the resistive model associated with the largest geoelectric field amplitudes and consequently with the most extreme GICs (Figure 4).

Scenario B (Figure 5) is the conducting model associated with a lower field amplitudes with the peak |E| = 5 V/km.

Pulkkinen et al. (2012) derived the models referring to the Canadian ground conductivity model. Strictly speaking, Canadian ground models cannot simply be applied to geomagnetic observations from different geographical regions. However, Pulkkinen et al. (2012) contend that excluding regions close to strong conductivity anomalies, to a good approximation the same magnetospheric current will produce similar total magnetic variations at regions with different ground conductivity structures.

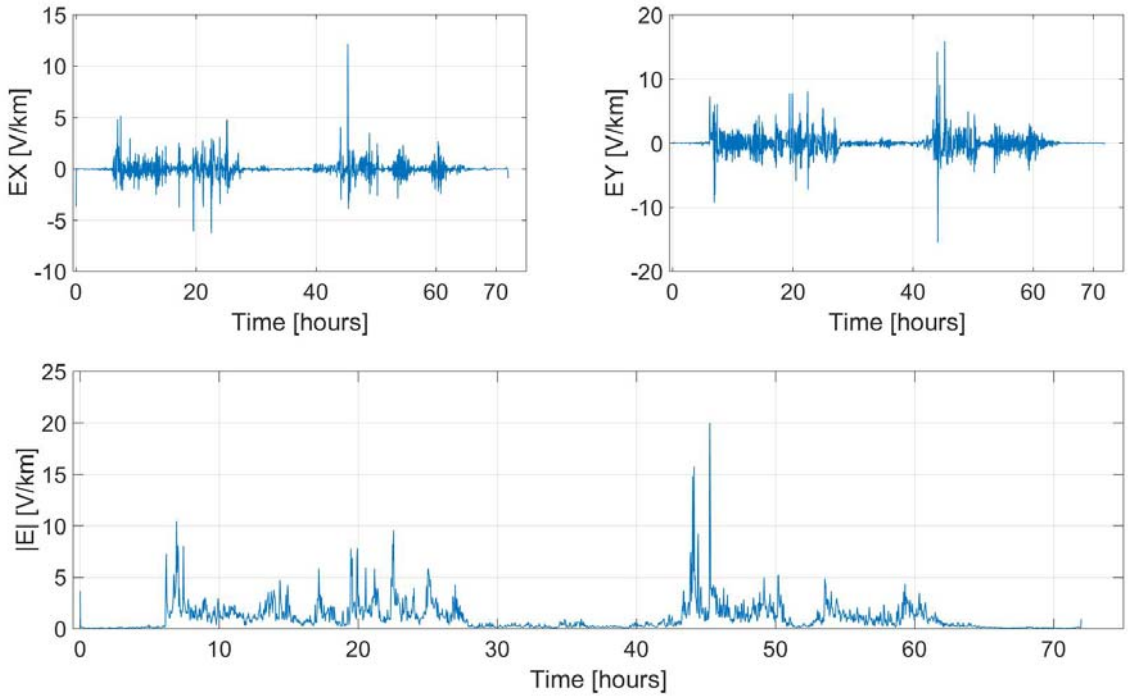

Figure 4. Scenario A for resistive ground structures located at high latitudes. The upper plot on the left represents the northward component of the geoelectric field (EX), while the upper plot on the right represents the eastward component (EY). The maximum geoelectric field amplitude is |E| = 20 V/km (bottom plot).

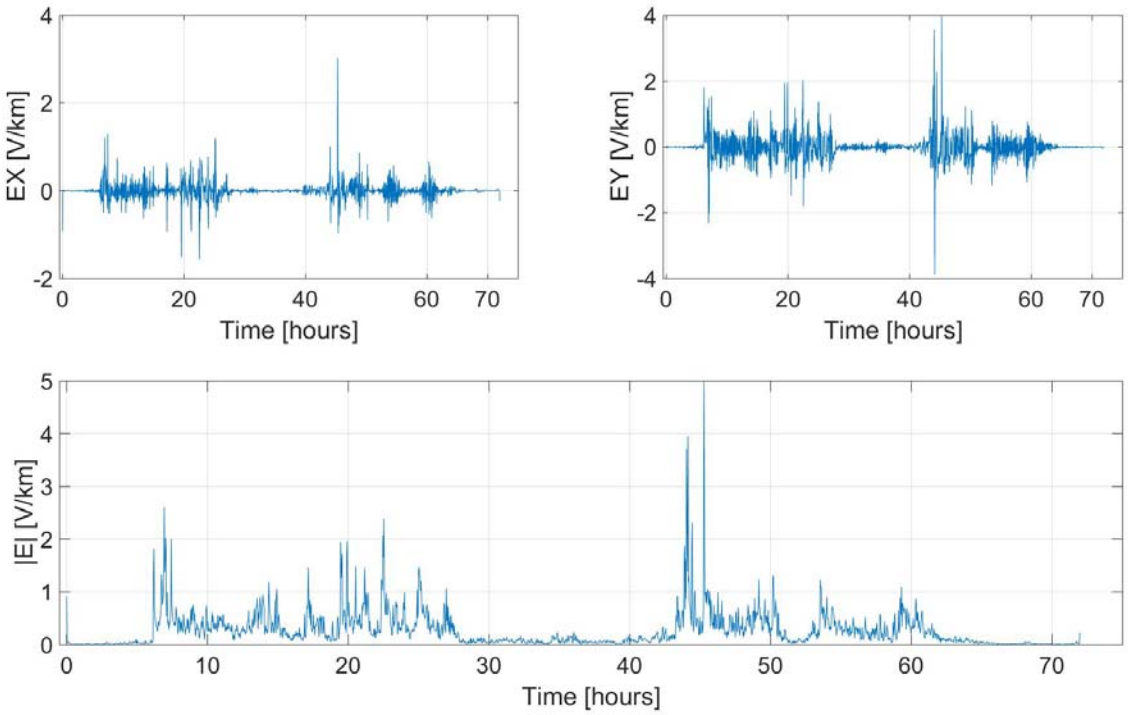

Figure 5. Scenario B for conductive ground structures located at high latitudes. The upper plot on the left represents the northward component of the geoelectric field (EX), while the upper plot on the right represents the eastward component (EY). The maximum geoelectric field amplitude is |E| = 5 V/km (bottom plot).

3.2 Transformer behaviour

To better understand how the variation in time and the variation of the direction of the field interacts with the behavior of the transformers in the network, we had to consider the behavior of the transformer from a different perspective.

Transformers are conceived and designed to operate in AC regime. When direct currents, such as GICs, enter, the transformer is driven into saturation zone. The reaction of the transformer due to saturation has been described by many simulation methods (Lu and Liu, 1991; Walling and Kahn, 1991).

These methods are usually accurate but they need detailed information that is not generally available.

To estimate the consumption of reactive power by the system, with only the given GICs and the nameplate information of the transformer, we adopt a simplified approach proposed by Dong (2002). We assume the following:

- The nameplate information of the transformer is known, including the rated voltage and MVA, that is the output that can be delivered without exceeding specified limitations;
- The input GIC is known and divides equally between the three phases;
- The AC and DC flux only flow in the core. Leakage flux is ignored.

Knowing the saturation curve of the transformer it is possible to calculate the reactive power consumption.

The magnetizing curves are usually represented using piecewise linear representations, as shown in Figure 6.

The coefficients k_i are the slopes of the lines: they represent the inductance of the transformer that is its behavior in non-saturation and in saturation regime. Ic_i is the current corresponding to the change of slope, also called the knee-point current. It can be seen that mono-phase transformers reach the saturation regime with lower levels of current, with respect to three-phase transformers. This explains their greater vulnerability to GIC impact. Experiments show that k, the empirical coefficient is equal to 2.8 for single phase transformers and 0.4 for three-phase three limbs transformers (Sokolova et al. 2014).

3.3 The Finnish power grid – Scoping study

In Piccinelli and Krausmann (2014), the 400 kV Finnish transmission grid model by Pirjola (2009) was adopted as benchmark model for the evaluation of GICs. On that occasion, a study of the topological properties of the system was proposed that aimed at highlighting how the structure of the system and its geophysical characteristics, e.g., the conductivity of the ground and the line lengths, may drive GICs into the system, eventually leading to collapse. A preliminary study of the behavior of the system in its operational mode was also carried out. A geomagnetic storm and subsequent GICs were considered in the power flow of the system.

Once GICs are calculated, the effects of geomagnetic disturbances on the system are determined. As presented in Section 2.2, GICs primarily influence power grids by inducing saturation in transformers. This entails a variety of effects, among which an increase in reactive power demand at the nodes in which transformers are located, is predominant. The increasing in load varies linearly

(Dong et al., 2001) with the GIC flowing in the transformer, so given the transformer specific constants k, the corresponding reactive power demand can be determined.

The conceptual scheme of the approach used is represented in Figure 7.

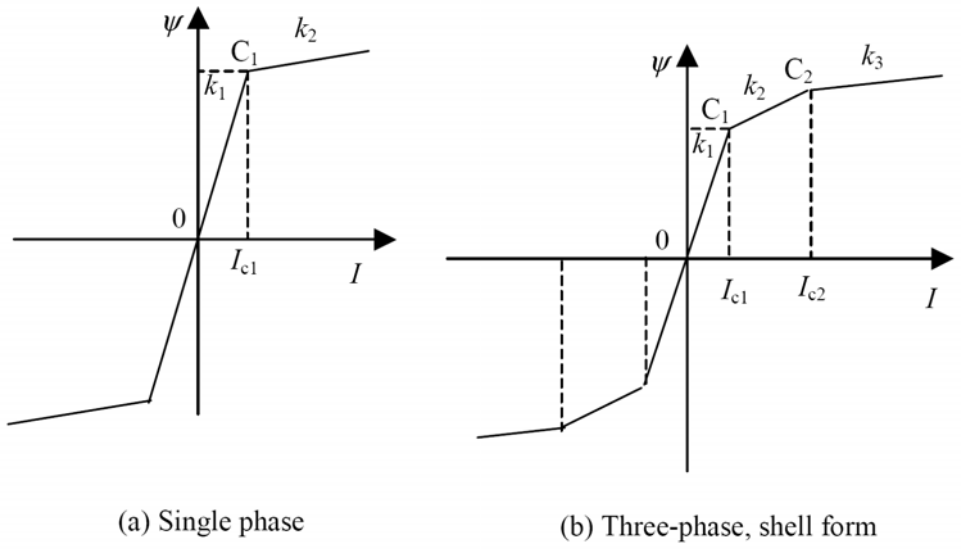

Figure 6. Representation of the equivalent magnetizing curve of the transformer (Dong, 2002).

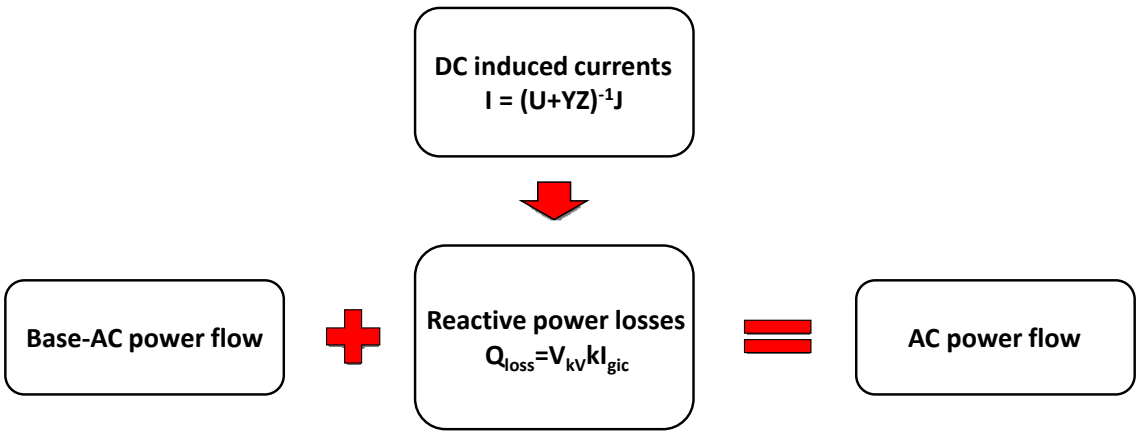

Figure 7. Outline of the method employed to evaluate the load flow in the 400kV transmission grid in the presence of GICs.

3.3.1 Static analysis

Simulations were conducted considering a transformer for every node of the network. Since no information is available on the exact distribution of transformers in the network, that is type and number of transformers, we considered two network configurations: 1) the worst case scenario, in which all transformers are mono phase, the most vulnerable type of transformers with respect to space-weather impact, and 2) a scenario in which all transformers are three phase.

For our scoping study, we considered four geomagnetic storm scenarios based on work by Pirjola (2002) and Pulkkinen et al. (2012). Starting from |E| =1V, a typical value of for a geoelectric field (Pirjola, 2002), in each scenario we increased the magnitude of the field: |**E**|=1V, 2V, 5V and 20V. We considered the peak intensities proposed by Pulkkinen et al. (2012) as the highest magnitudes for the electric field. For each of these electric field magnitudes and for each 15-degree field orientation from 0 to 165 degrees, the resulting AC power flow was calculated using MATPOWER (2011). System collapse was assumed to have happened when the power flow calculation did not converge. The results for the *mono-phase scenario* are summarized in Table II.

	0	15	30	45	60	75	90	105	120	135	150	165
|**E**|=1V												
|**E**|=2V												
|**E**|=5V												
|**E**|=20V												

Table II. Schematic representation of the convergence of the power flow algorithm for the Finnish 400-kV power transmission grid as a function of electric field strength and orientation and assuming that all transformers are mono-phase. Red boxes indicate grid collapse.

The voltage affecting the line depends on the electric field and on the projection of the length of the transmission line parallel to the direction of the electric field. We kept the geoelectric field magnitude uniform, therefore the varying contribution to the voltage is given by the projection of the "global length" of the network. Since the geometry of the network extends more in the northward than the eastward direction, a strong geoelectric field directed northward is expected to have a more pronounced impact on the network, in agreement with the results of our analysis.

For the scenario in which we assume all transformers to be three phase, our simulations show convergence of the power flow. This indicates that the benchmark Finnish 400 kV grid model is resistant to GIC impacts under the assumed conditions of electric field strength and orientation.

3.3.2 Dynamic analysis

Geomagnetic storms vary with time. In order to assess the behavior of the power system under such conditions, the same analysis as in section 3.3.1 was carried out but considering time-dependent GMS scenarios. The maximum absolute values of the electric field for the different scenarios were the same as in the static analysis. Each value of the electric field was sampled at intervals of 10 seconds.

For the purpose of the dynamic analysis, we considered the time-varying scenarios A and B (presented in Section 3.1) and two network configurations, with only mono-phase or only three-phase transformers. For each time step of the varying electric field, we considered the transformer to saturate instantaneously and applied the same simulation method outlined in Figure 7. We obtained convergence of the Finnish benchmark grid system for both GMS scenarios and both network configurations. This seems to indicate that the Finnish power grid is robust against geomagnetic storm impact, both if we consider only mono-phase or three-phase transformers. The benchmark power grid appears to be robust against solar storms even with the highest intensities of the electric field and this result confirms the evidence that up to now Finland has not experienced any failure due to geomagnetic storms (Lahtinen and Elovaara, 2002).

A possible explanation is that during dynamic scenarios, the geoelectric field varies its magnitude and direction with time. The latter in particular changes randomly, so it may happen that the angle between the directions of the line of the system and the electric field may not give rise to GIC formation and hence reactive power demand from the system, which increases the risk of voltage collapse.

GICs result from the interaction between the geoelectric field and the transmission lines: their orientation to each other influences the GIC magnitude. Since this interaction is expressed by a scalar product, the more the electric field and the lines are aligned, the higher will be the generated GICs.

Statistically, in the chosen scenarios, the east-west direction is the most probable direction for the geoelectric field. We focus the attention on the Scenario A with the highest peak intensity. Figure 8 shows the histogram representing the distribution of the electric field orientations for Scenario A. Most of the GMS events have direction angles included between ± 30 degrees where zero is the reference point for the east-west direction.

Transmission lines in the Finnish benchmark power grid are distributed along the different directions. Figure 9 shows that only 23% of the lines falls into the [-30, +30] degree interval. This means that the orientation of the grid is such that the effect of the GMS is limited in spite of high electric field intensity values.

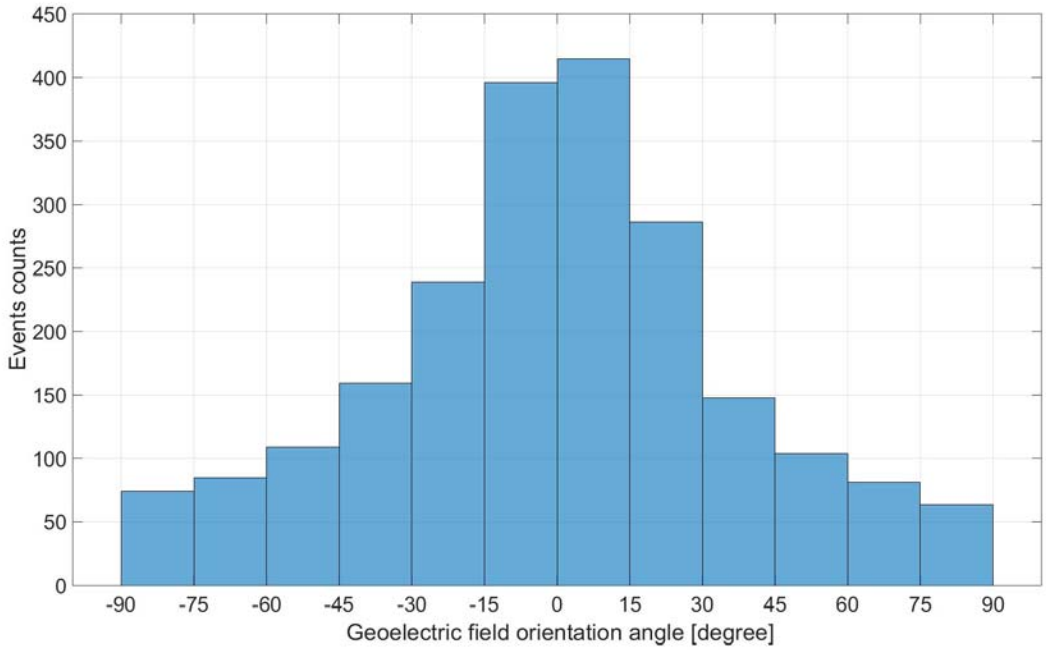

Figure 8. Histogram representing the distribution of the orientation angles of the time varying geoelectric field for Scenario A (the time varying components of the geoelectric field EX and EY are shown in Figure 4). Zero is the reference point for the East-West direction.

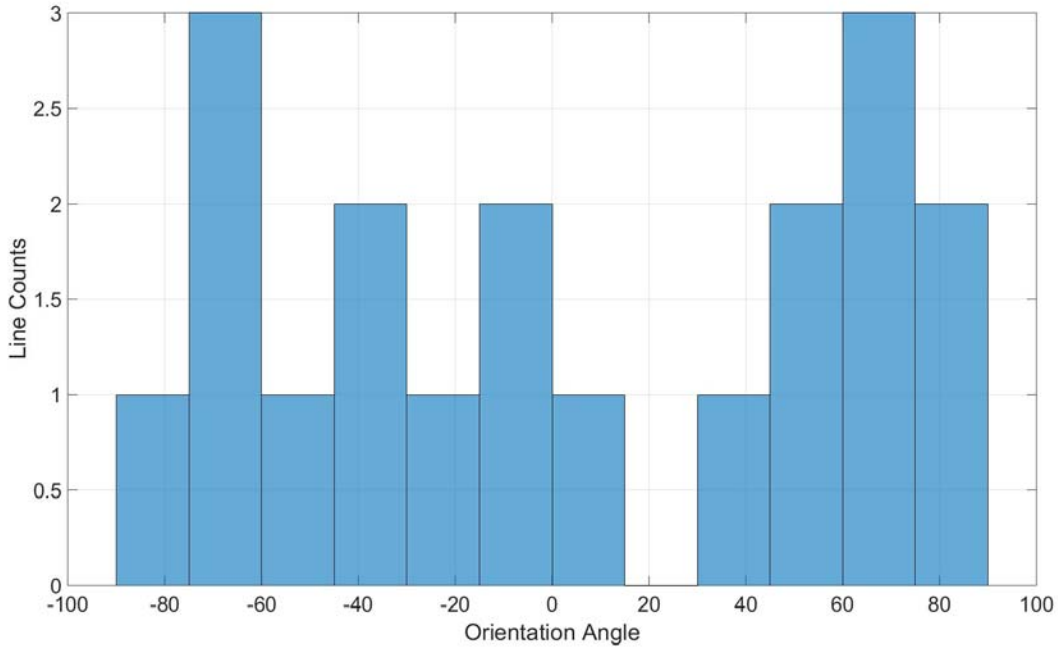

Figure 9. Histogram representing the distribution of the orientation angles of the transmission lines of the benchmark Finnish power grid.

3.4 The Scandinavian interconnected power grid

The Finnish study was extended to analyze the vulnerability to space weather of a power transmission grid model that extends over the Scandinavian region and comprises the 400kV lines-network of Norway, Sweden and Finland. The 17-node benchmark model introduced by Pirjola (2009) and used in section 3.3is embedded in the extended Finnish part of the grid. The full network consists of 147 stations and 200 transmission lines and each station is assumed to include a transformer.

3.4.1 Power grid model and assumptions

Finland, Sweden, and Norway compose the northern part of the European power transmission grid. While there have been efforts to model the continental European power grid (Zhou and Bialek, 2005), to our knowledge there are no models for the Northern European part of the grid that are publicly available. The only public information is available from the network topology map of the European Network of Transmission System Operators for Electricity (ENTSOE) shown in Figure 10 (ENTSOE, 2015). Using the data extracted from the map, we also needed data on power generation or power demand for our analysis. Since these data are available only as cumulative data for total power generation and demand, we used population census data energy quantities to estimate the generation and demand on the different parts of the grid, as previously done for the Finnish power grid (Piccinelli and Krausmann, 2014). In accordance with Zhou and Bialek (2005), we considered the household power demand proportional to the population density.

The power generation in Scandinavia is very heterogeneous in both electricity sources and geographic distribution of generation. Norway relies to 99% on hydro power for its electricity generation (SSB, 2015; Statkraft, 2015). Most hydropower plants are located in the southern part of

Norway. Sweden has a mix of hydropower, nuclear and other thermal power plants (SCB, 2015; SEA 2015). Most hydropower plants are located in the middle and in the north of Sweden. Finland also has hydropower plants in the north but also relies on other thermal power plants (FINGRID, 2015; Statistics Finland, 2015).

Figure 10. Map of the Scandinavian 400kV power grid. Transmission lines are approximated by straight lines, while stations are represented by nodes (ENTSOE, 2015). Each node is assumed to represent a transformer.

Most of the population lives in the southern part of the Scandinavian Peninsula. This is a fundamental aspect of the topology of the network, especially with respect to the length of the transmission lines. As it can be seen from Figure 11, the average length of the transmission lines is 88.5 km, the longest lines being located in the central part of the network, corresponding to Sweden where generation plants are at a greater distance with respect to Finland and Norway.

The line length of the network is an important parameter for GIC assessment, since the voltage that gives rise to geomagnetically induced currents is projected along the lines. Two topological line parameters are fundamental for the evaluation of the geoelectric field generated by the GMS: the length of the line and the line orientation angle, which determines the projection of the geoelectric field along the line. The longer the line and the closer the alignment between the line and the orientation angle of the geoelectric field, the higher will be the voltage generated by the geoelectric field, and therefore, the higher will be the current induced in the power system.

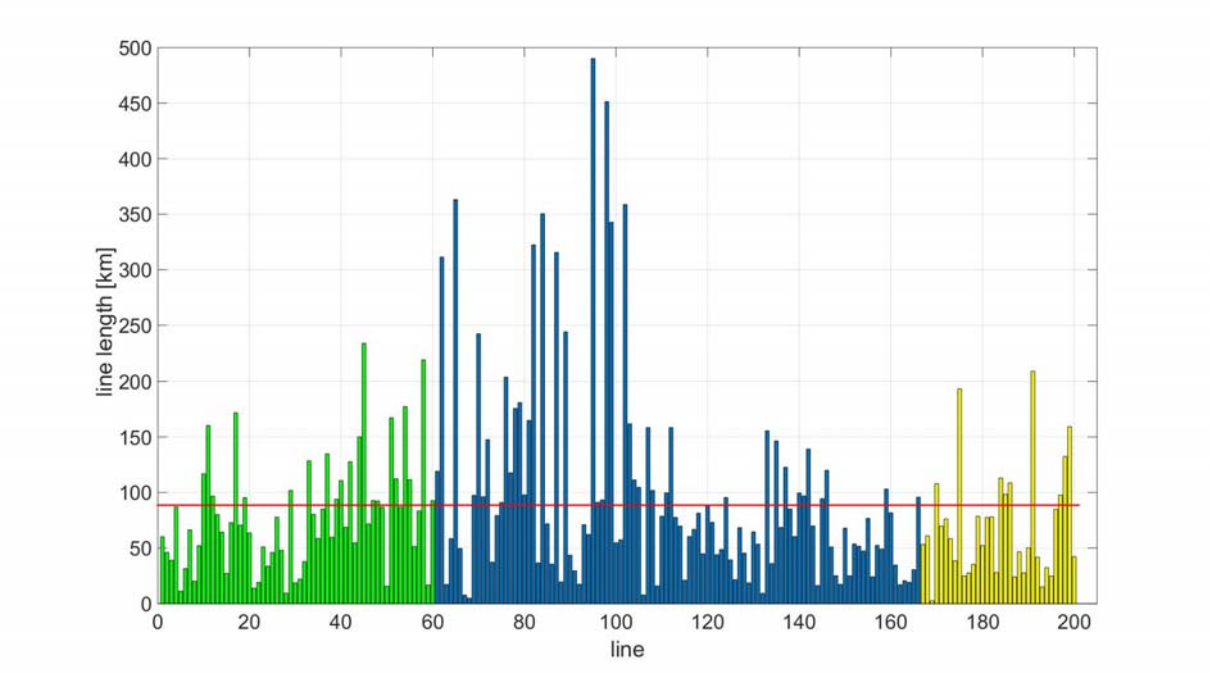

Figure 11. Line lengths for the Scandinavian interconnected power transmission grid are represented with different colors: Finland is represented in green (line 1 to line 60), Sweden in blue (line 61 to line 166) and Norway in yellow (line 167 to line 200). There are only few very long lines, with lengths greater than 300 km, all of which located in Sweden. The longest line measures 490 km.

The orientation of the transmission lines in the Scandinavian interconnected power grid is shown in Figure 12.

Only 33% of the lines falls into the [-30, +30] degree interval, that is the interval in which the majority of the electric field orientation angles are concentrated (Figure. 8). Therefore, based on the orientation of the grid we would expect no pronounced GMS effects.

Similarly to our simulations for the benchmark model of the Finnish 400 kV-power grid, we assumed the line resistances per unit length to be 0.008 Ω/km for 400 kV lines (Viljanen et al., 2012). In addition, all the stations only have one transformer.

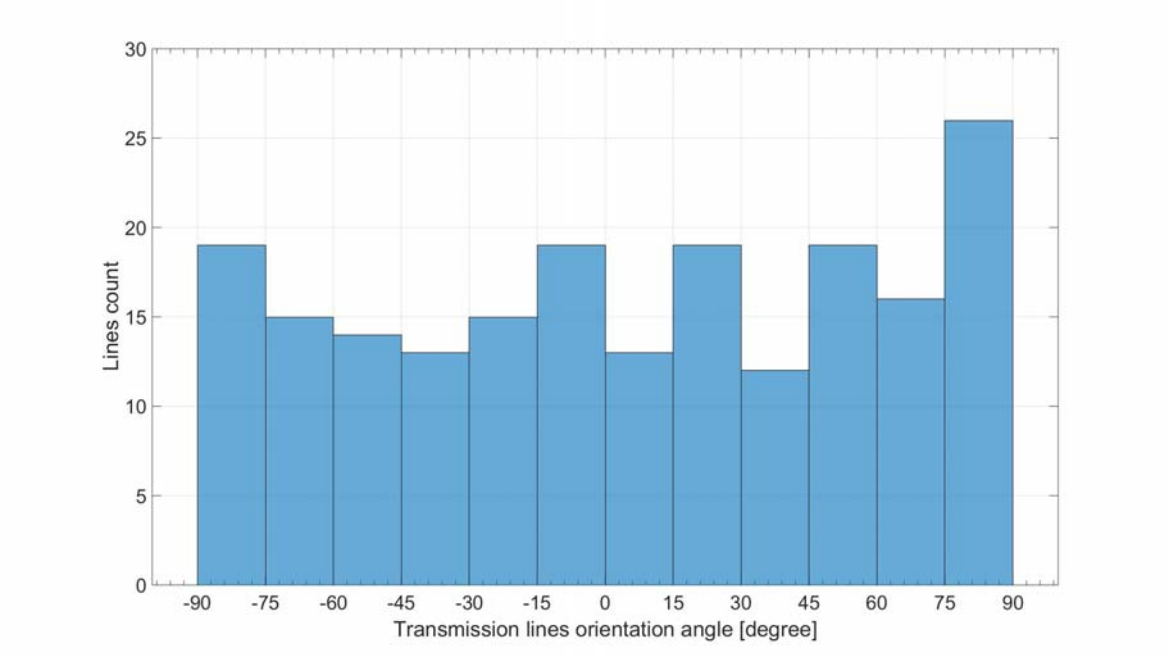

Figure 12. Histogram representing the distribution of the orientation angles of the transmission lines of the Finnish, Swedish and Norwegian power systems.

3.4.2 Simulations

In our simulations we consider only the two time-varying high latitude scenarios of Pulkkinen et al. (2012), which are the two scenarios with the highest geoelectric field peak values in Table I: Scenario A ($|E|_{peak}$ = 20 V/km) and Scenario B ($|E|_{peak}$ = 5 V/km).

The first step is the assessment of GICs in the system according to the different scenarios. For each time variation of the geoelectric field (Figure 4), the system experiences varying GICs flowing through nodes and lines. Since GIC values are proportionally scaled with the electric field (Pirjola, 2008), we can equally consider one of the two scenarios to understand how GICs spread throughout the system. Values ranging from 1 to 7 V/km have been measured in the Scandinavian region (Wik et al, 2009), so in Figures 13 and 14 we refer to scenario B with a geoelectric field intensity $|E|$ = 5 V/km.

According to the results of our simulations for Scenario B, the highest values of GICs are of the order of 200 A: the highest induced current (254 A) is located at node 147 situated in Norway (Figure 13) and located at the edge of the system where nodes exhibit larger GIC levels. This result agrees with the work carried out by Pirjola (2002) and Viljanen and Pirjola (1994). The direction of GIC flows has no relevance on their impact: both directions may drive transformers into half-cycle saturation (Bernabeu, 2013). These results also agree with observations reported in Pulkkinen et al. (2008) according to which GIC amplitudes of several hundreds of ampere and geoelectric field magnitudes of the order of 10 V/km are possible, although rare.

Figure 14 shows the induced currents through the transmission lines of the power system. In the specific example, the longest lines spread the highest currents through the system, because they happen to be aligned with the geoelectric field. This also verifies the statement that induced currents in transmission lines are generally clearly larger than those through nodes (Pirjola, 2002), in which transformers are located.

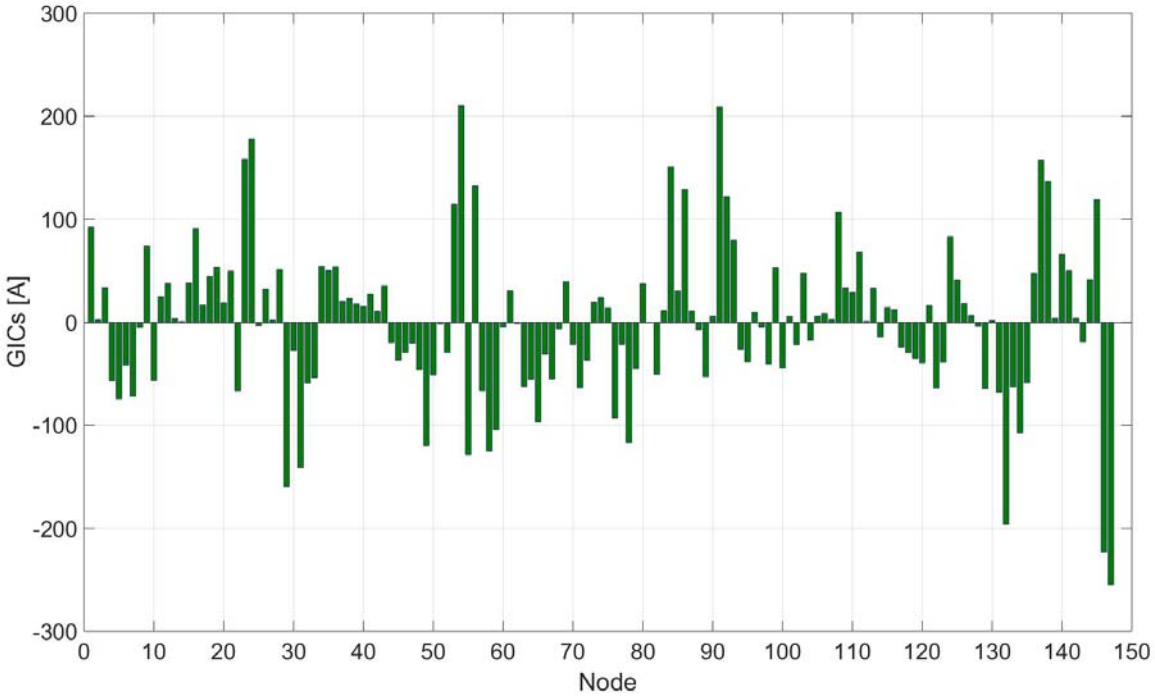

Figure 13. Representation of GIC computed for scenario B when the |E|= 5 V/km. The sign of the currents refers to the direction of the flow at the stations of the network: positive values are GICs exciting the nodes of system while negative values are GICs entering the nodes of the system.

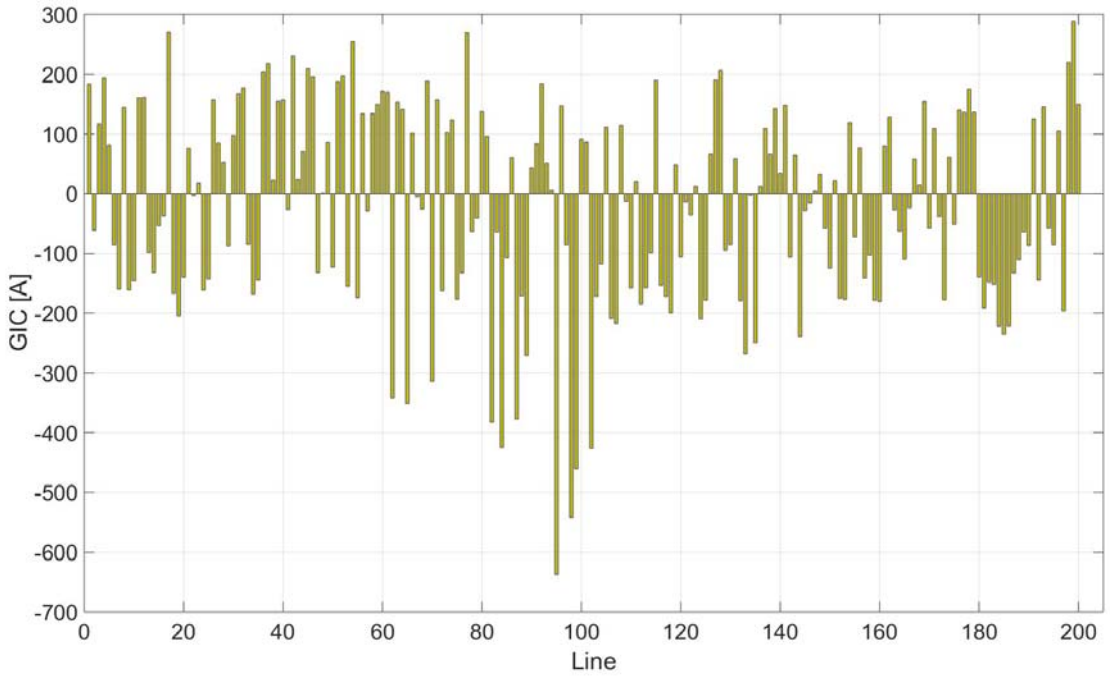

Figure 14. Representation of GIC flow through the lines of the network when |E| = 5 V/km. The sign refers to the orientation of the flow: in a transmission line connecting two nodes, e.g. node 1 and node 2, positive values suggest that GICs flow from node 1 to node 2; negative values suggest that GICs flow the opposite way, from node 2 to node 1.

GIC values are proportionally scaled with the electric field, so in case of Scenario A we have the same trend for GICs at nodes and lines, but with higher intensities. In case of extreme events with $|E|_{peak}$ = 20 V/km our results indicate that GICs values at nodes and lines of the grid are increased fourfold. Once again, the node with the highest GIC is node 147 (1,019 A) at the edge of the network, and the line with the highest computed GIC (2,500 A) is line 95, located in Sweden. These extremely high values are the result of assuming a worst-case scenario for the electric field.

3.4.2.1 Power flow

The direction of the geoelectric field and the orientation of power lines affect GIC at different locations of the system, but the dependence is complicated by the fact that GIC induced in one part of the grid may flow to another. Therefore, it is important to consider how GICs interact with the power flow within the system.

The base case for the AC power flow consists of the network load configuration obtained from the statistical data (as described in Section 3.4.1) considered in the absence of any geoelectric induced field, that is when |E| = 0 V/km. Calculations were implemented using the MATPOWER software (MATPOWER, 2011).

Figures 15 shows the voltage magnitudes (per unit, p.u.) for the 147 buses of the Scandinavian interconnected transmission network, during operational mode (AC power flow), that is in the absence of any GMS.

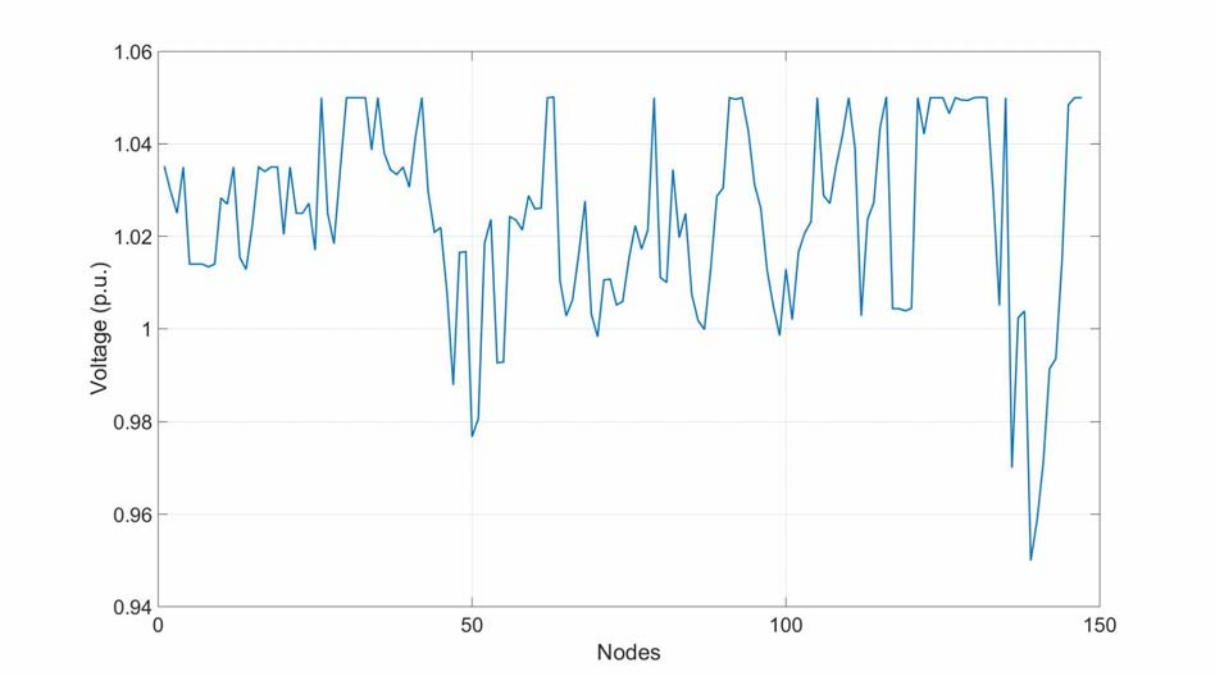

Figure 15. Bus voltage magnitudes during ordinary operational mode (when |E| = 0 V/km) based on network load configuration estimated from the data described in Section 3.4.1. The voltage ranges from V_{min} = 0.95 p.u to V_{max} = 1.05 p.u.

Figure 16 shows the reactive losses experienced by the transmission lines during ordinary operational mode. Voltages and reactive losses for the base case of the AC load flow scenario will serve as a comparison for the behavior of the system during an extreme space-weather event.

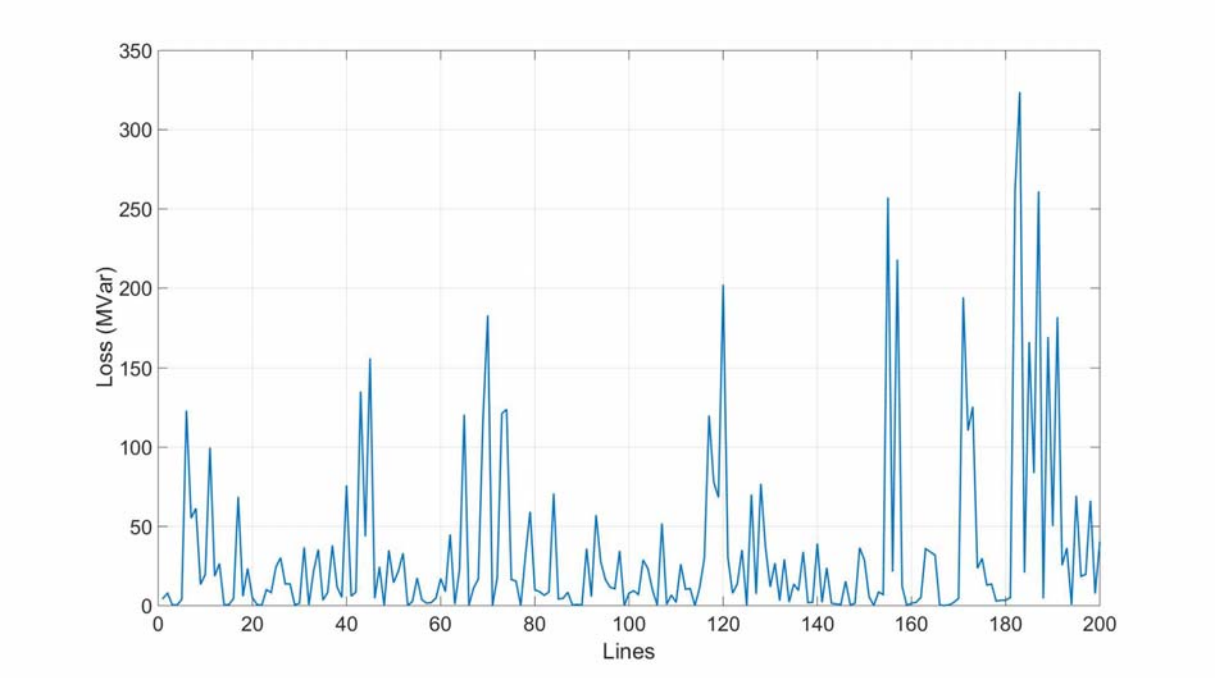

Figure 16. Transmission line losses of reactive power during ordinary operational mode (when |E| = 0 V/km).

In Section 3.4 we already discussed that the Scandinavian interconnected network has generating units concentrated in few sites. Therefore, lines connecting the power plants directly to the grid transmit high power flow and register the highest losses during normal operations.

In our analysis, for each scenario we run the AC power flow for the power network considering two different types of transformers. Since there is no public information on the distribution of each type of transformer in each station of the network, we consider two configurations of the network. They represent two extreme cases: one case, in which all transformers are mono phase, or the most vulnerable type, and one in which all transformers are three phase, which is a configuration more resistant to GICs.

For both system configurations and for each Scenario A and B an AC power flow simulation was conducted as described in Figure 7. We ran the power flow simulation for each time step, corresponding to the 10-second interval of the geoelectric field measurement. Where transformer saturation was observed, we considered the transformer to saturate instantaneously. This is the most conservative assumption for transformer behavior (Bernabeu, 2013). After each step, we assumed that the system resets to an unsaturated configuration. There are two possible results: the power flow converges, which means that the system withstands the GMS or the power flow does not reach convergence, which means the system experiences a collapse.

3.4.2.2 Case a) System with mono-phase transformers

The network configuration with only mono-phase transformers is the worst-case assumption in terms of vulnerability of the network, since all transformers are of a type that is known to be strongly affected by GMS. Our simulations ran for the two GMS Scenario A and B, and the results show that the system appears to resist a Scenario B-type geomagnetic storm. Non-convergence for the system, that is collapse of the system, occurred only for Scenario A for which we registered 33 collapse events. Figure 17 shows the magnitudes of the electric field during the 33 collapse events.

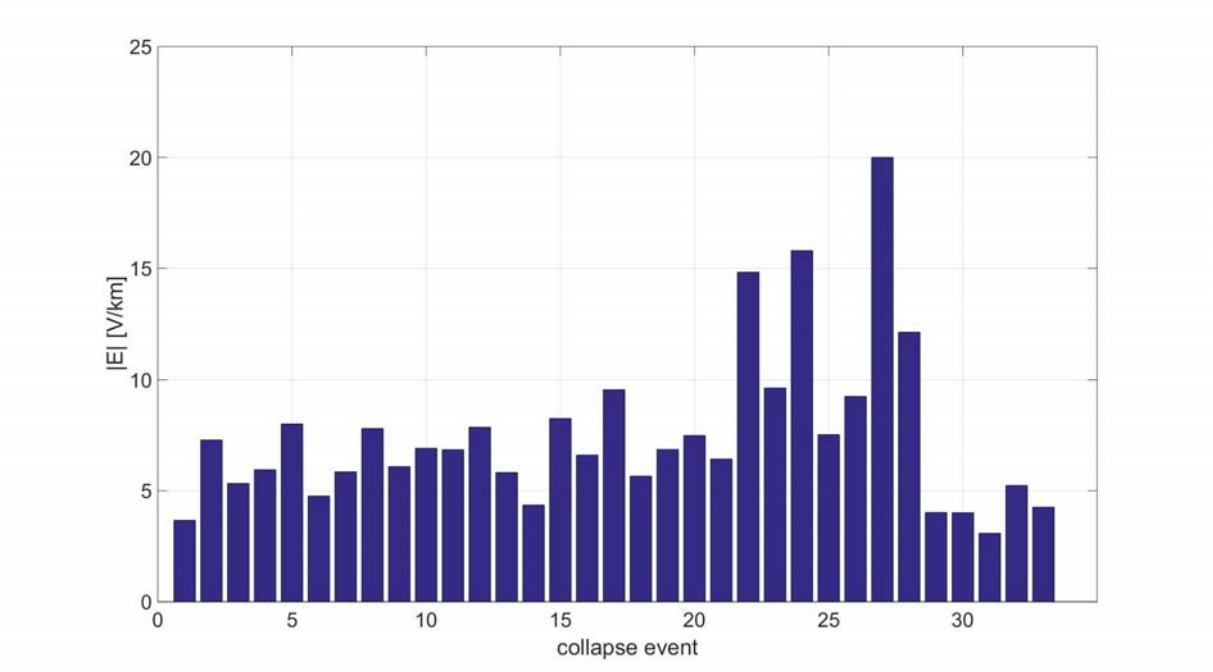

Figure 17. Representation of the magnitudes of the geoelectric fields of Scenario A, for which the system with mono-phase transformers collapses.

For each collapse event, we estimate the variation in the bus voltages, the GIC distribution at nodes and the reactive losses in lines. Among the 33 events, we consider in detail two collapse events: the event of collapse corresponding to the lowest value of geoelectric field that is |E| = 3.08 V/km (Figure 18) and the event corresponding to the peak value of the electric field, i.e. |E| = 20 V/km (Figure 19).

During AC power flow, electric power is distributed throughout the network so that the nodes' requested load can be supplied. Voltage magnitudes at nodes adjust in order to meet the supply. A collapse event can happen when the system experiences a significant voltage change throughout the nodes of the network. In Figure 18, the voltage[1] drop induced by the GMS (red line) cannot be overcome to restore the voltage needed during normal operation (blue line). It can also be seen that some nodes require high voltage intensity (red line above the blue line), but the system is unable to supply it and therefore collapses.

If we compare the voltage magnitudes during the event with the lowest geoelectric field value that leads to collapse, |E| = 3.08 V/km, and the peak value |E| = 20 V/km (green), (Figure 19), we still observe a generalized voltage drop throughout the nodes of the system.

It is interesting to observe the magnitudes of GICs at the nodes of the network during the two considered collapse events (Figure 20). The figure shows the nodes at which GICs enter the system, but then the power flow drives them through the network. Not always nodes that experience the highest GICs suffer from the worst voltage drop.

[1] The per-unit system (p.u.) is used in power system analysis to express values of voltages, currents powers and impedances of power equipment as fractions of a defined base quantity. In this report, we express voltage at nodes in (p.u) and relate voltage values to the base quantity of 400 kV.

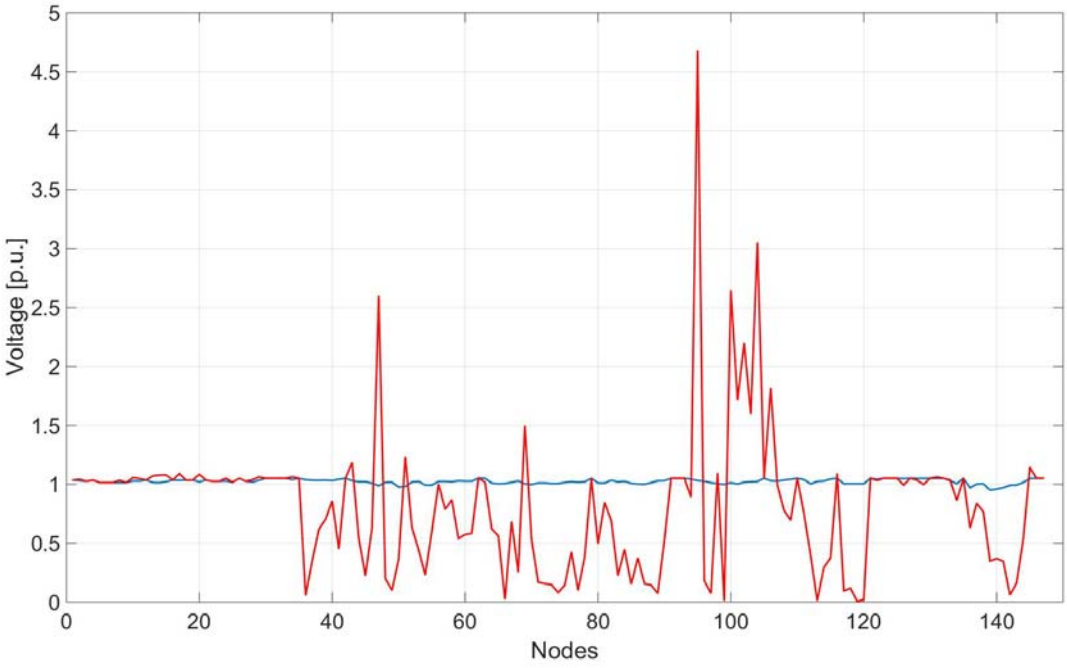

Figure 18. Voltage magnitudes at the buses of the Scandinavian interconnected power network for the base case, |E| = 0 V/km (blue) and during the first event of collapse, |E| = 3.08 V/km (red).

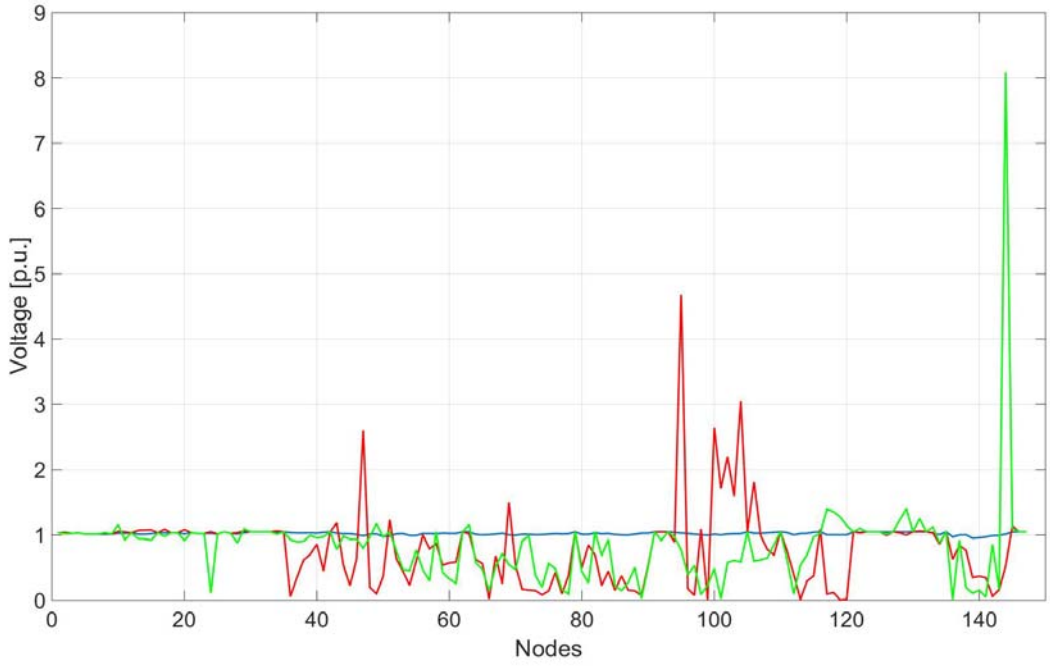

Figure 19. Voltage magnitudes comparison at the buses of the Scandinavian interconnected power network for the base case, |E| = 0 V/km (blue), during the first event of collapse |E| = 3.08 V/km (red) and during the peak value event, |E| = 20 V/km (green).

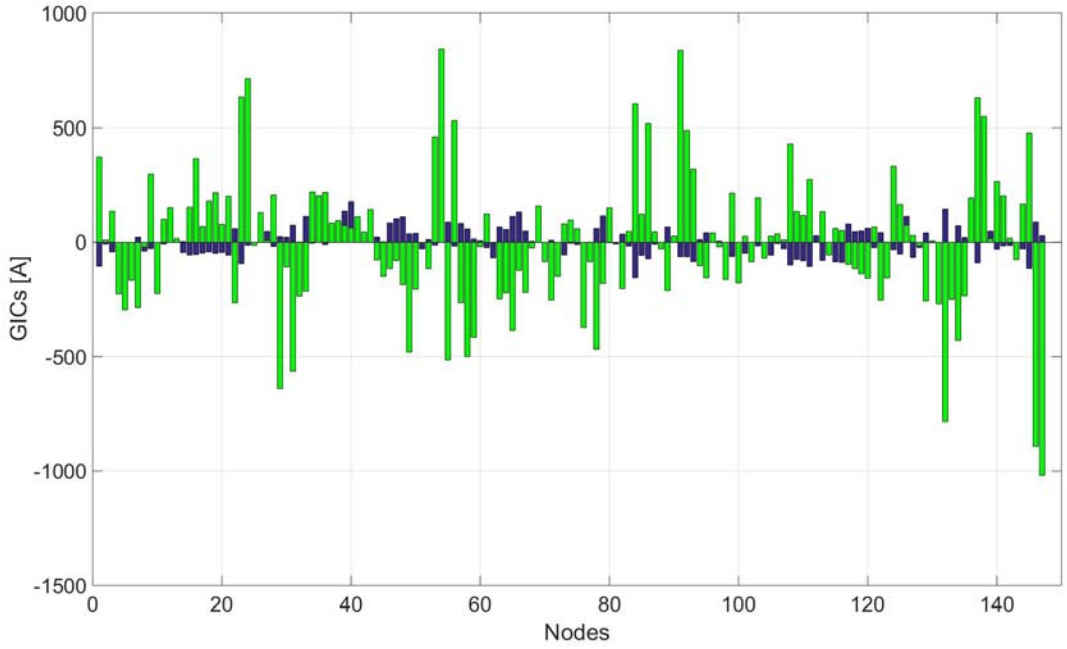

Figure 20. Comparison between GIC computed for scenario A, when |E|= 3.08 V/km (blue) and when |E| = 20 V/km (green). The sign of the currents refers to the direction of the flow at the stations of the network: positive values are GICs exiting the nodes of system while negative values are GICs entering the nodes of the system.

Figure 21 shows the reactive losses on lines during the base case and during the event of collapse corresponding to a field magnitude of |E|= 3.08 V/km. The highest losses correspond to the lines connecting power plants that deliver a high quantity of power to the system. The highest peak of reactive loss in Figure 21 corresponds to the line connecting to one of the biggest power plants in Sweden (1600 MW).

Finally, Figure 22 shows that the highest reactive losses in transmission lines when |E| = 20 V/km correspond to the lines showing the highest losses also in the base-case scenario in the absence of an electric field (Figure 16). They are also the lines connecting the nodes with the highest geomagnetically induced currents (Figure 20).

The last point to be analyzed concerns the intensity of the electric field during collapse. Our simulations indicate that no collapse occurs for Scenario B, which is characterized by a field peak value of |E| = 5 V/km. This may appear odd considering that for Scenario A several collapse events happen for |E| values lower than 5 V/km. Figures 23, 24 and 25 compare the voltage, GICs and reactive losses for the case |E| = 3.08 V/km from Scenario A with the case |E| = 5 V/km from Scenario B. It can be clearly seen that the higher intensity of the geoelectric field induces the highest GICs in the system (Figure 24) but this is not a sufficient condition for the system to collapse. An important factor that contributes to determining if a system can withstand voltage drops is the interaction between the power flowing throughout the network and the effects of increased superimposed reactive power demand on the power flow. If the reactive power demand due to currents induced by the GMS allows the system to supply power within voltage and loss constraints at nodes and lines, the system is able to function and no collapse event is registered. On the other hand, if the reactive power demand happens to nodes and lines already working in the proximity of

limiting conditions, the system may not be able to fill the gap between its reactive generating capacities and the increased reactive power demand generated by GICs, causing its collapse.

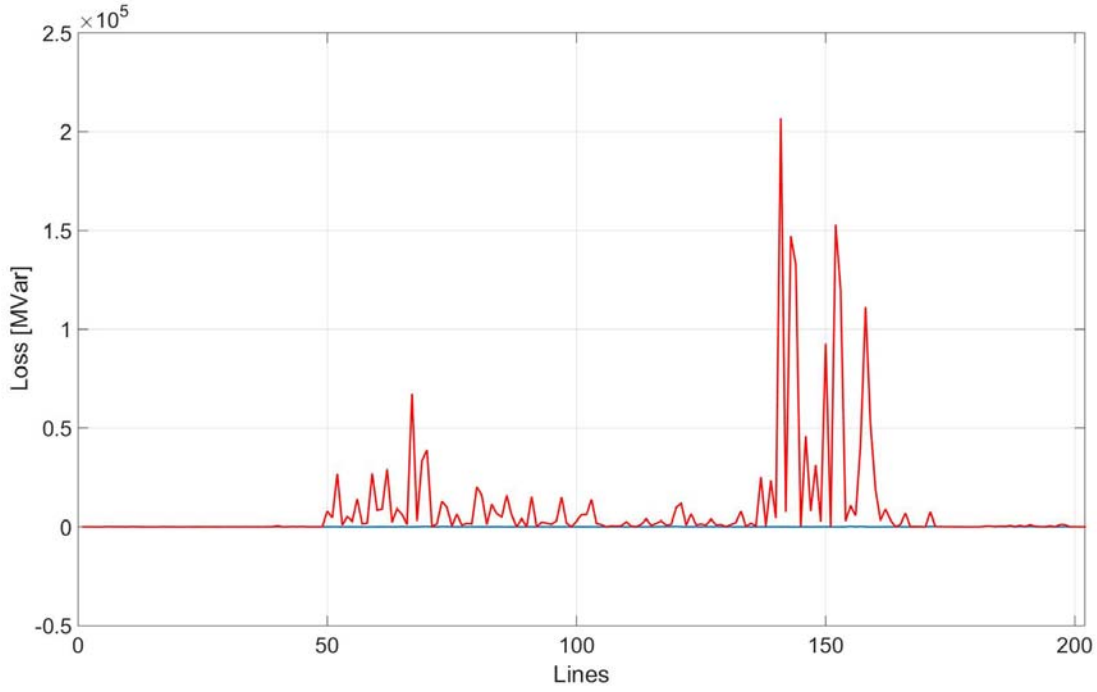

Figure 21. Transmission line losses of reactive power during ordinary operational mode (when |E| = 0 V/km) and during the first event of collapse, |E| = 3.08 V/km (red) (the unit of reactive losses is MVar or Mega Volt Ampere Reactive).

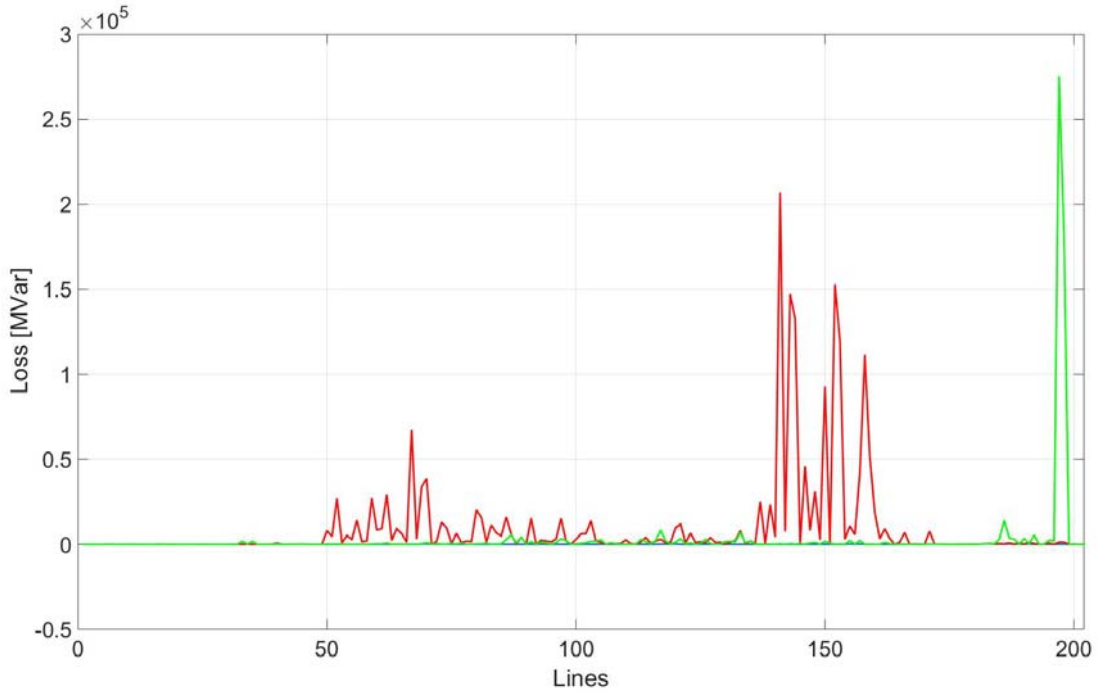

Figure 22. Comparison of transmission line losses of reactive power during ordinary operational mode (when |E| = 0 V/km), during the first event of collapse, |E| = 3.08 V/km (red) and during the peak value event, |E| = 20 V/km (green).

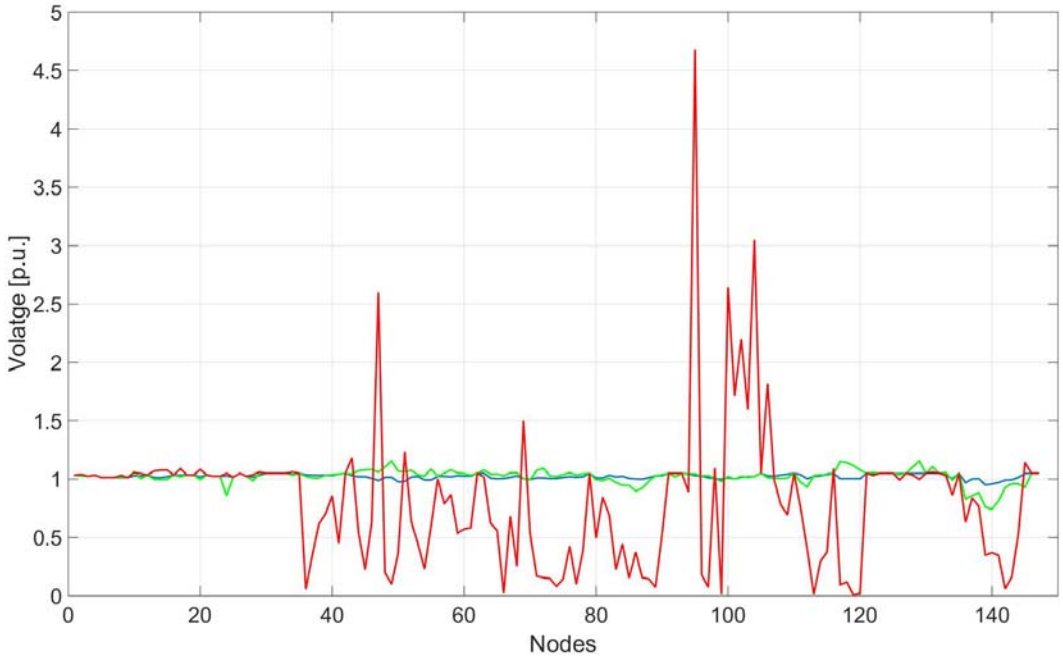

Figure 23. Voltage magnitudes comparison at the buses of the Scandinavian interconnected power network for the base case, |E| = 0 V/km (blue), during event of collapse |E| = 3.08 V/km (red) of Scenario A and during the peak value event, |E| = 5V/km (green) of Scenario B.

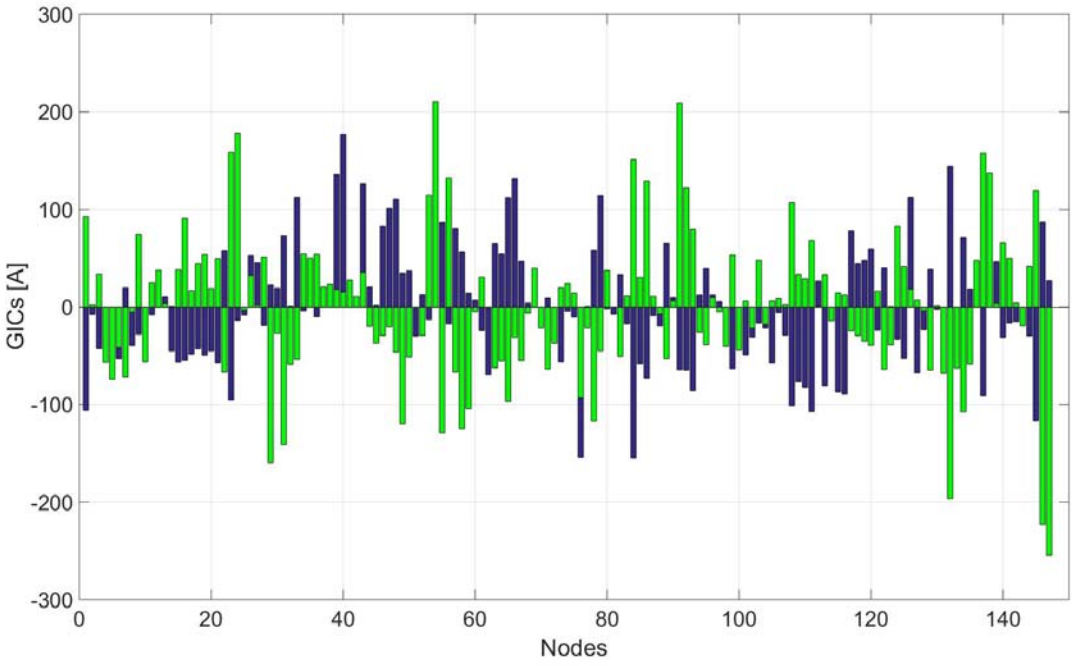

Figure 24. Comparison between GIC calculated for Scenario A, when the |E|= 3.08 V/km (blue) and the GIC for Scenario B, when |E| = 5 V/km (green). The sign of the currents refers to the direction of the flow at the stations of the network: positive values are GICs exciting the nodes of system while negative values are GICs entering the nodes of the system.

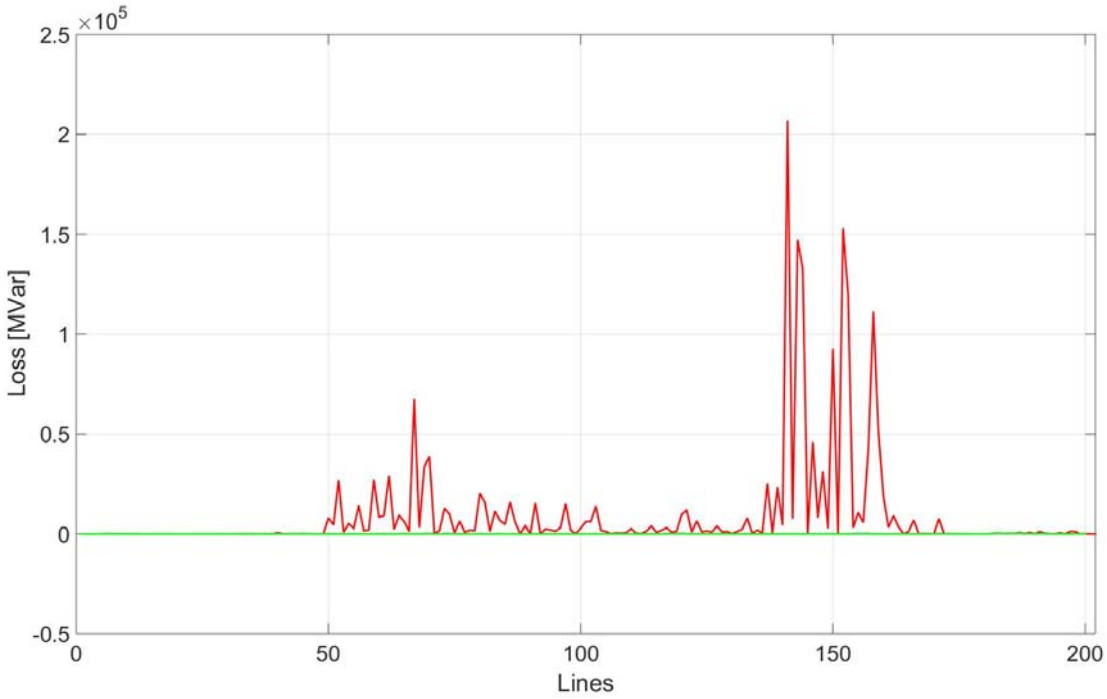

Figure 25. Comparison of transmission line losses of reactive power during ordinary operational mode (when |E| = 0 V/km), during the first event of collapse, |E| = 3.08 V/km (red) for Scenario A, and during the peak value event, |E| = 5 V/km (green) for Scenario B.

The overall results on voltages, GICs at nodes and losses for the 33 collapse events are summarized in Figures 26, 27 and 28 respectively.

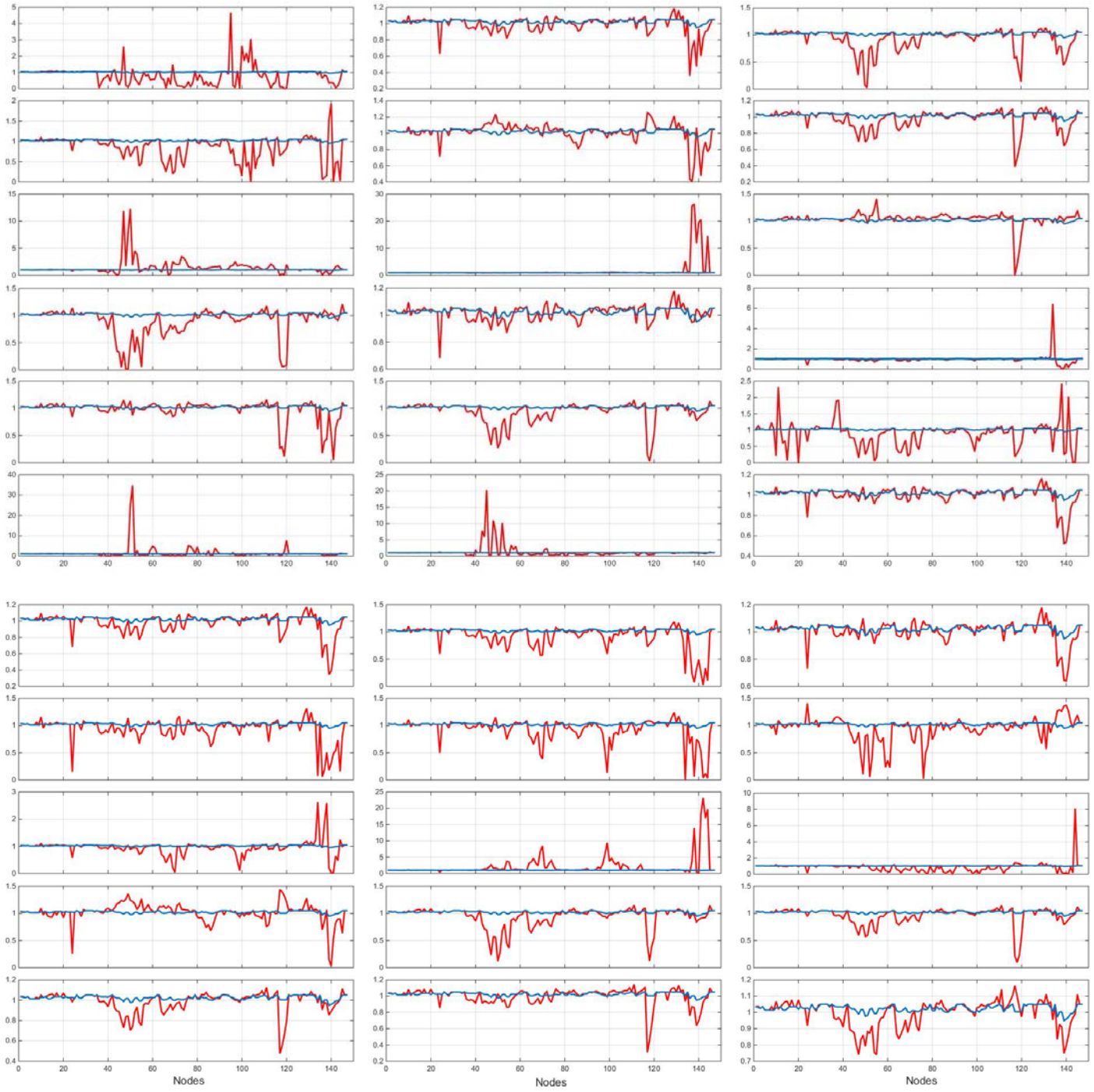

Figure 26. Bus voltage variations during the 33 collapse events for Scenario A. Each rectangle represents an episode of collapse. Bus voltages (on the y axis) are expressed in p.u. for every node of the system (x axis). The blue line represents the bus voltage, when there is no GMS, while the red line shows the voltage variations due to the GMS. Note that the vertical scales vary in the different subplots.

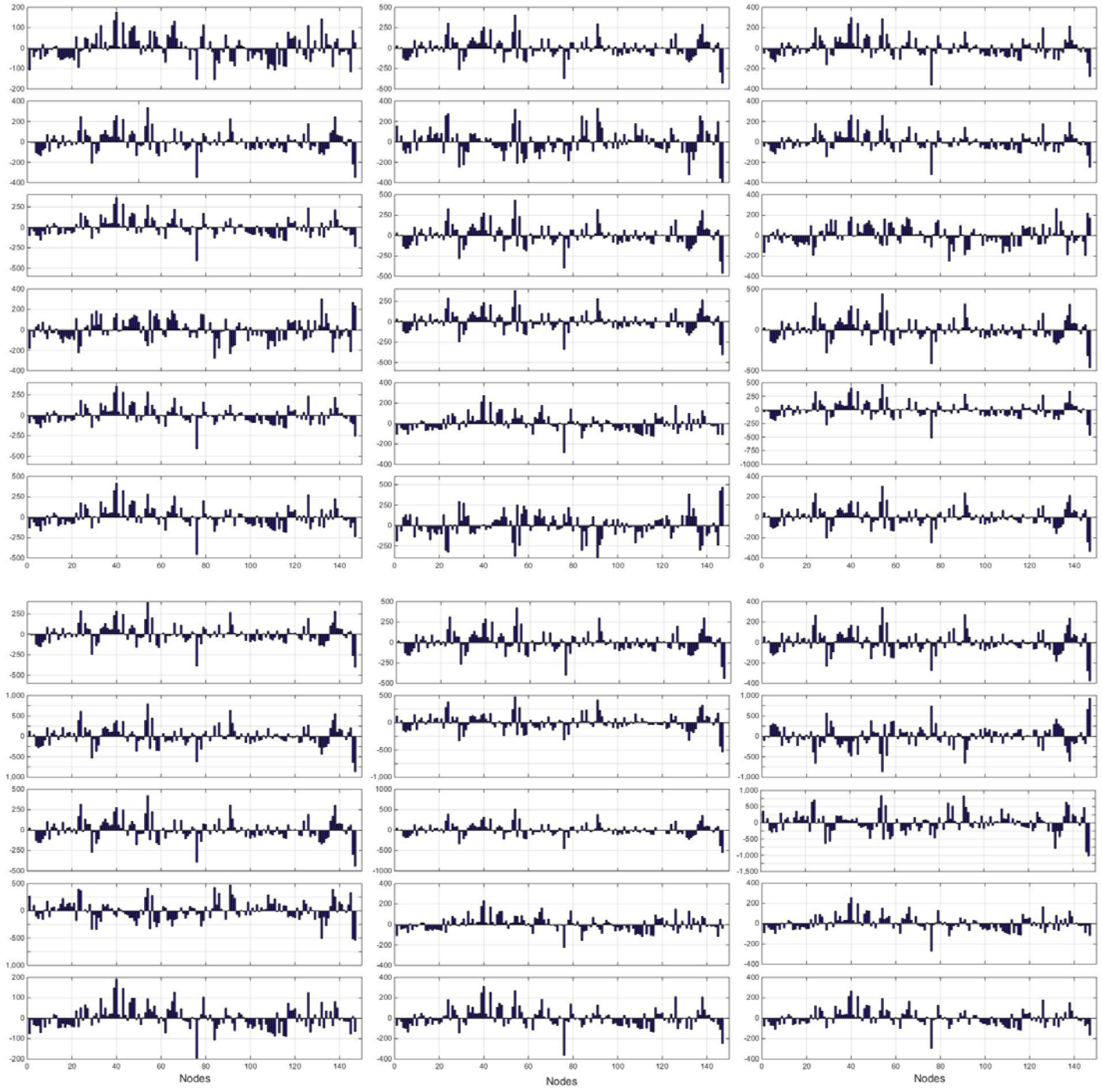

Figure 27. Representation of GIC values in the network nodes for each collapse event in the system for Scenario A. GICs, on the y-axis, are expressed in Ampere for every node. Note that the vertical scales vary in the different subplots.

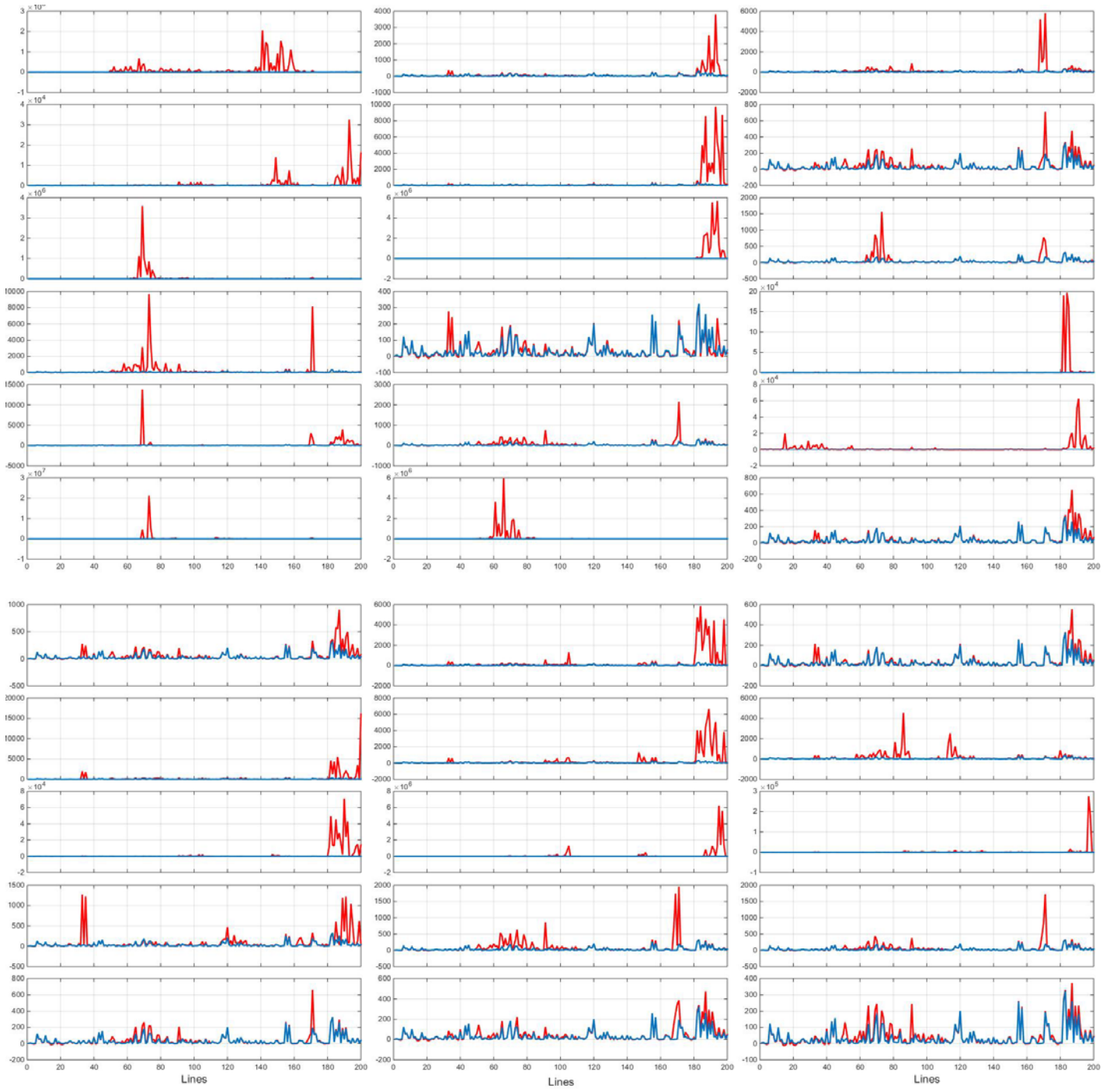

Figure 28. Representation of the reactive losses in the lines. Each rectangle is an episode of system collapse for Scenario A. The reactive losses, expressed in MVar on the y-axis, are represented for each line. The variation of the reactive losses during normal operational conditions (in blue) are represented against the variations caused by the GMS (red line). Note that the vertical scales very in the different subplots.

3.4.2.3 Case b) System with three-phase transformers

The network configuration comprising three-phase transformer collapsed only in two events of scenario A. For both cases, the magnitude of the geoelectric field was extremely high. As expected, no collapse occurred during our simulation for the conditions of Scenario B. This is consistent with the observation that three–phase transformers are less vulnerable than mono-phase.

The first collapse occurred when |E| = 14.8 V/km. Figures 29, 30 and 31 illustrate the trend for voltage, GIC at nodes and the losses of reactive power in lines.

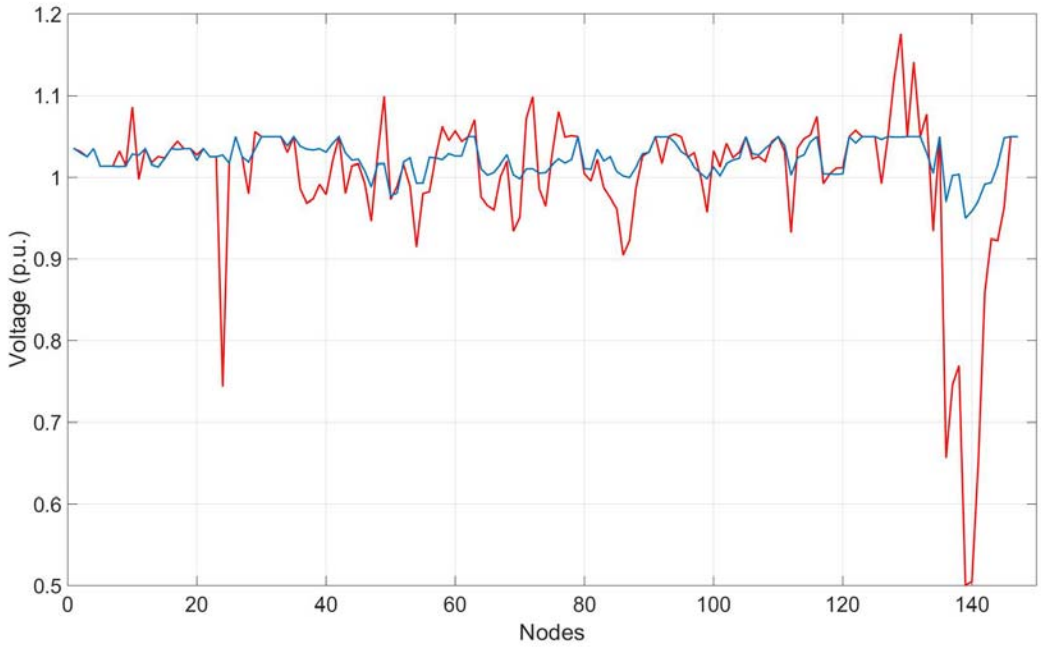

Figure 29. Bus voltage magnitudes for the base case with no GMS (blue) and in the presence of an electric field with magnitude |E| = 14.8 V/km.

As can be seen from Figure 29, the system experiences a drastic voltage drop with respect to the base case. The nodes, and thus the transformers most affected by the GMS are situated in the southern part of Norway at nodes 139 and 140. The related GICs per phase, featured in Figure 30, show that high values of induced currents are also present in other parts of the grid, for example at node 55 or at node 147.

The second case of collapse for the three-phase transformer configuration of the network is the extreme event, corresponding to the highest geoelectric intensity |E| = 20 V/km. Figures 32, 33 and 34 show the behavior of the power system in such an event. In this case, the system experiences very high values of voltage (Fig. 32) at the nodes and also high intensity of GIC currents (Fig. 33). In this case, the lines register huge values of reactive loss which is characteristic for significant voltage collapse risks (Figure 34).

The losses of reactive power on the lines indicate that in case of |E| = 20 kV/km, the central lines corresponding to Sweden, which are the longest ones, suffer from extremely high losses. For |E| = 14 kV/km, the lines at the end of the graph, i.e. the lines corresponding to Norway, are the most affected by reactive power loss (Figure 34).

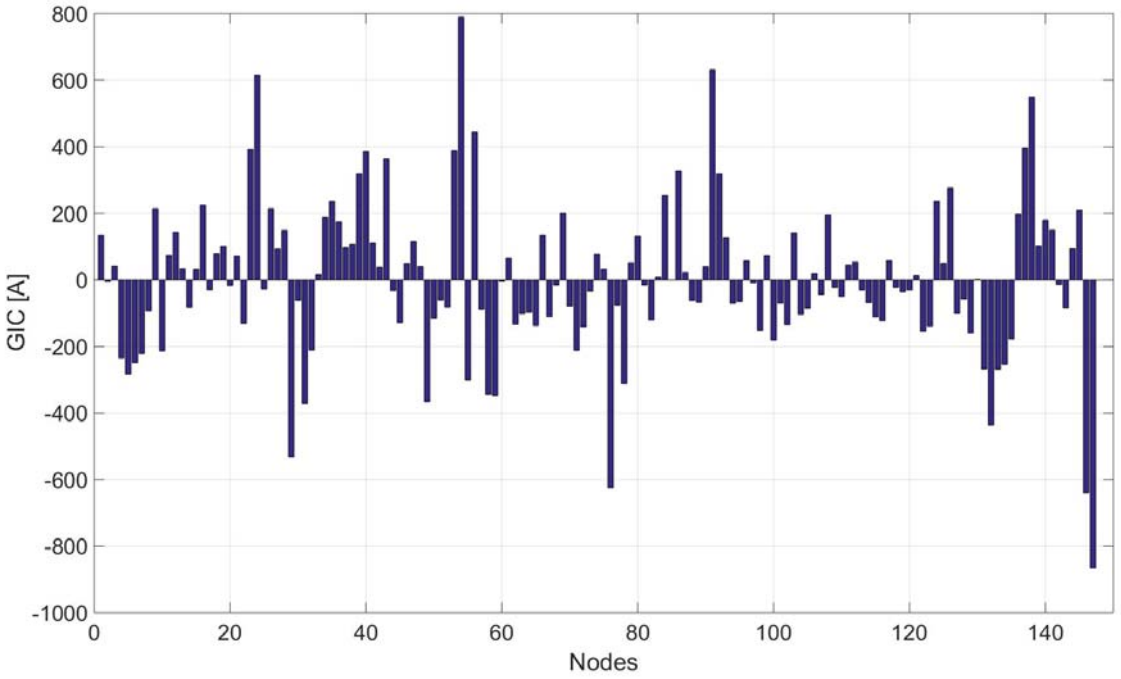

Figure 30. GIC per phase in the nodes of the Scandinavian network when the geoelectric field intensity is |E| = 14.8 V/km.

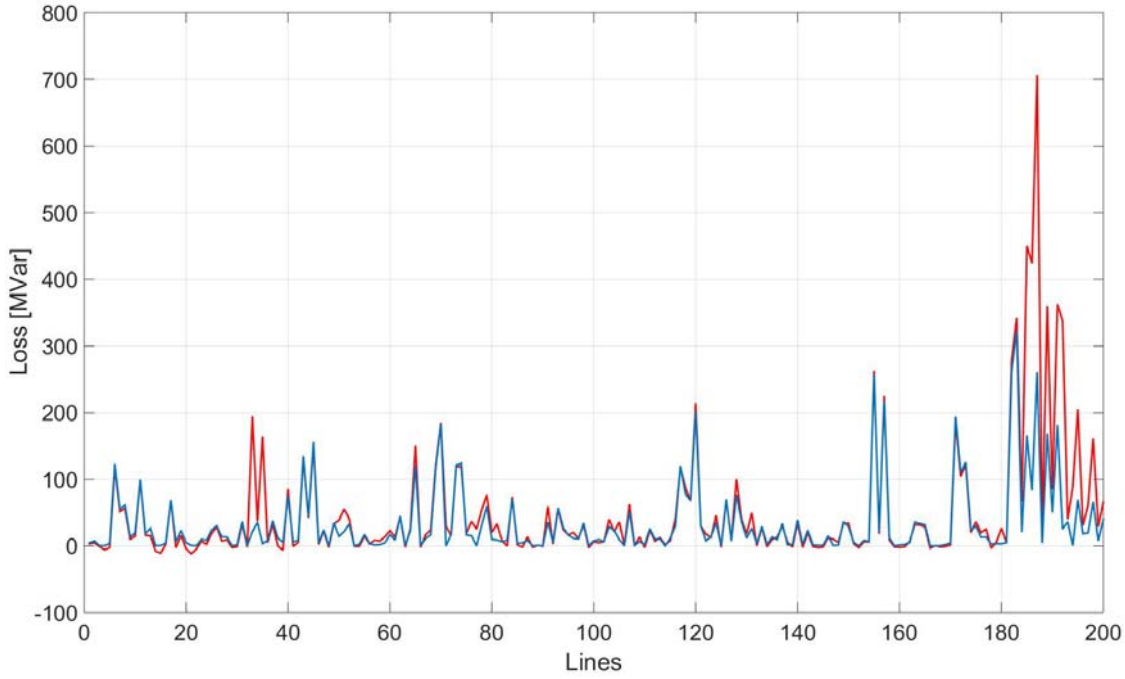

Figure 31. Reactive power losses in the transmission lines when the geoelectric field magnitude is |E| = 14.8 V/km (red line) compared with line reactive power losses during normal operation regime, when |E| = 0 V/km (blue).

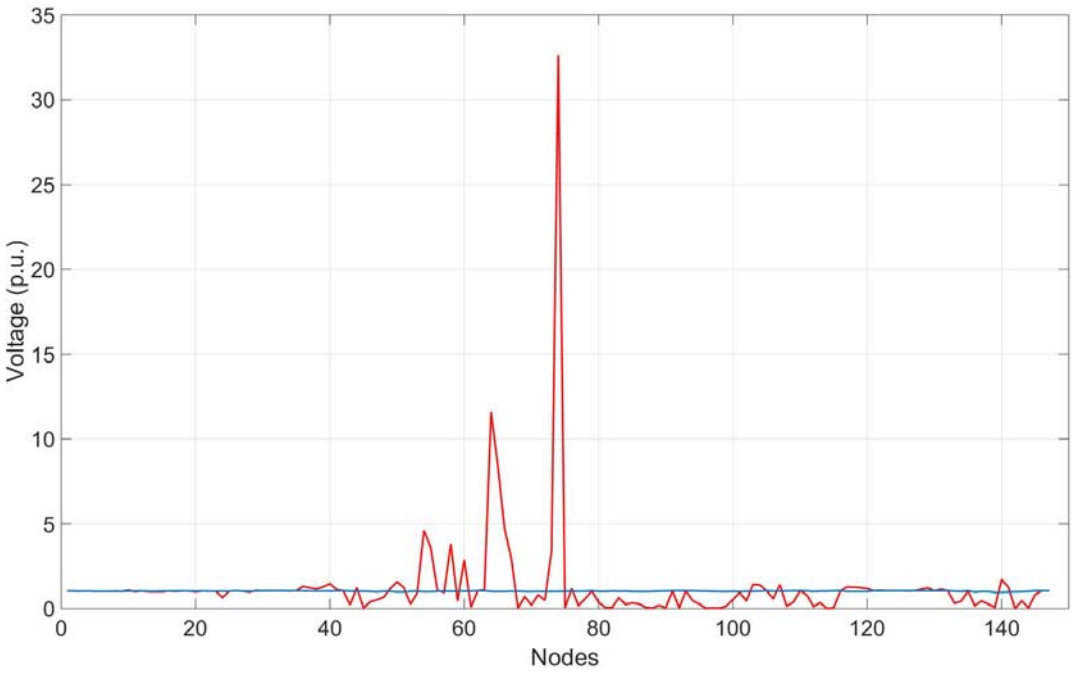

Figure 32. Bus voltage magnitudes for base case (blue) and for the electric field with magnitude |E| = 20 V/km. This is the highest intensity considered in the benchmark scenario developed by Pulkkinen et al. (2012).

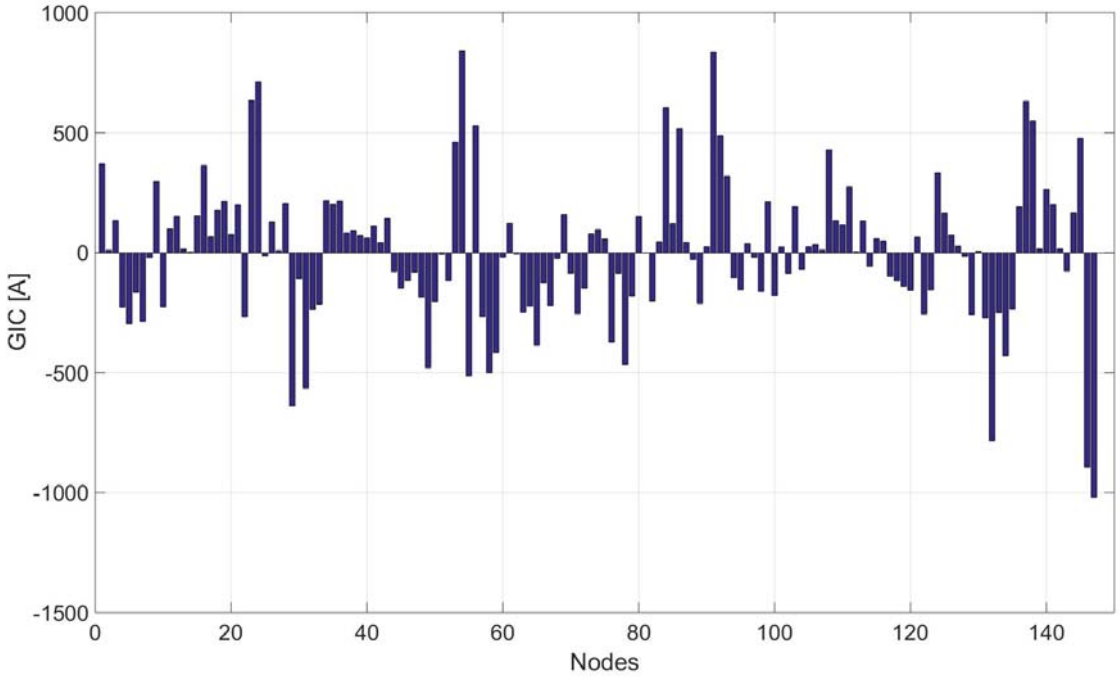

Figure 33. GIC per phase in the nodes of the Scandinavian Network when the geoelectric field intensity is |E| = 20 V/km.

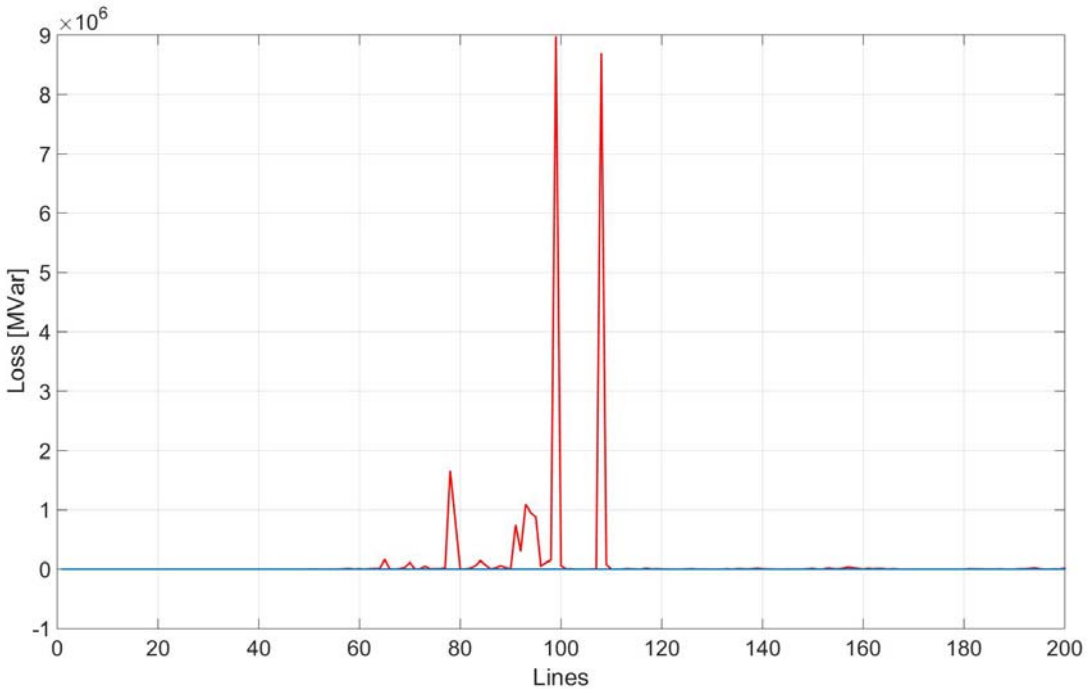

Figure 34. Reactive power losses in transmission lines when the geoelectric field magnitude is |E| = 20 V/km (red line), and reactive power losses in transmission lines during normal operations, i.e. |E| = 0 V/km (blue line).

4. Discussion and conclusions

Power grids can suffer outages or blackouts during geomagnetic storms. Transformers were identified as the most vulnerable components of the power networks: geomagnetically induced currents cause transformers to work in saturation regions generating voltage instability and eventually driving the system to collapse.

In this report we extended our analysis from a scenario with uniform geoelectric field intensity to a time-varying scenario applied to the Scandinavian 400 kV interconnected power transmission grid. For this purpose we choose two extreme space-weather benchmark scenarios proposed in the literature.

For our simulations we had to make some assumptions on the power grid model in the absence of detailed data. We assumed that every node of the grid includes a transformer of one of two different types: either transformers of the mono-phase type, the most vulnerable, or three-phase transformers, the most reliable type. We also did not consider any kind of protection system in place. We then calculated the GICs induced by the GMS scenarios to identify the nodes at which the system will experience the highest GICs. However, these GICs flow throughout the system obeying the power flow laws and to understand their impact on the network it is necessary to superimpose an AC power load flow to simulate the normal operating conditions of a power network. For this purpose, we considered a base-case load flow, representing one possible ordinary operational configuration of the system.

Our simulations showed that the three-phase configuration of the network is significantly more robust than the mono-phase one. In case of extremely high electric field intensities (> 14 V/km) the system with mono-phase transformers collapses. Also the three-phase configuration is prone to collapse albeit with a much lower likelihood. For such an extreme event, the increase in reactive

power demand caused by transformer saturation is too high for the system to continue to provide power. For electric field values below 14 V/km our study shows that the system with the three-phase transformer configuration is robust and no collapse occurs, while the mono-phase configuration is extremely vulnerable to GMS. In this latter case, it is shown how the power flow drives the voltage instabilities through the system: lines that experience higher losses during normal operation, for example lines connecting the nodes with a high concentration of power plants in the system, are more likely to increase losses during a GMS event and to drive the system towards collapse. According to our study, the portion of the Scandinavian interconnected power transmission grid most vulnerable to extreme space weather is the part where the highest reactive losses in transmission lines and in voltage magnitudes are observed. This corresponds to the southern parts of Sweden and Norway.

As already indicated, for our study we had to make a number of simplifying assumptions to compensate for the lack of data especially on the power-grid configuration, but also to keep the simulations manageable from a computational point of view. Our primary assumption concerning transformer type and distribution in the grid should be revisited if detailed information becomes available as it is unlikely that every node includes one transformer and that transformer types are the same throughout the entire network. In a realistic network there will be nodes with multiple transformers and different transformer designs. Considering only one- or three-phase transformers, our current study analysed two extreme cases with worst-case and best-case assumptions. Along the same lines, load-flow regimes different from the base case could be modelled. A more realistic network configuration can be implemented easily into our analysis should the data become available. Transformer ageing due to cumulative space-weather effects, as well as the impact of harmonics in the network are also not commonly modelled.

In the near future this study will be extended to assess the risk of extreme space weather for larger portions of the EU power grid. In the medium term this work will also feed into the Joint Research Centre's Global Resilience and Risk Assessment Platform (GRRASP) which we will use to estimate cascading effects to Society due to potential power-grid failure by extreme space weather and its interdependencies with other types of critical infrastructure (Azzini et al., 2014).

Acknowledgements

The authors are grateful to Gianluca Fulli, Catalin-Felix Covrig, Arturs Purvins and Michel Vandenbergh of the JRC Institute for Energy and Transport for providing guidance concerning stability of the AC power flow. The authors would also like to thank Ivano Azzini and Marco Dido of the Critical Infrastructure Protection group at the JRC Institute for the Protection and Security of the Citizen for computational support.

5. References

Albertson V.D., Thorson J.M., Clayton R.E., and Tripathy S.C., Solar-induced-currents in power systems: cause and effects, *IEEE Transactions on Power Apparatus and Systems*, PAS 92, 2, 471-477, 1973.

Azzini I., Piccinelli R., Dido M., Krausmann E., and Giannopoulos G., Geomagnetically Induced Currents and Power Grids: A case study using GRRASP, *JRC Science and Policy Report JRC90792*, European Union, 2014 (Limited Distribution).

Boteler, D.H., Assessment of geomagnetic hazard to power systems in Canada, *Natural Hazards*, 23, 101-120, 2007

Dong X., Study of power transformers abnormalities and IT applications in power systems, *PhD Thesis*, Virginia Polytechnic Institute, 2002.

Dong X., Liu Y and Kappenman J., Comparative analysis of exciting current harmonics and reactive power consumption from GIC saturated transformers, *Proceedings from Power Engineering Society Winter Meeting*, 2001.

ENTSOE 2015, https://www.entsoe.eu last accessed 22th October 2015.

EPRI, How to calculate Electric Fields to determine Geomagnetically Induced Currents, *Technical update 3002002149*, Electric Power Research Institute, 2013.

Erinmez I. A., Majithia S., Rogers C., Yasuhiro T., Ogawa S., Swahn H., and Kappenman J. G., Application of modelling techniques to assess geomagnetically induced current risks on the NGC transmission system, *paper presented at Int. Counc. On Large Electr. Fields*, Paris, 2002.

FEN, Research Centre for Energy Networks – ETH Zurich, Geomagnetically induced currents in the Swiss transmission network, *A technical study commissioned by the Swiss Federal Office of Energy and Swissgrid*, 2013.

FINGRID, http://www.fingrid.fi last accessed 25th October 2015

IEEE, Working Group on Geomagnetic Disturbances, Geomagnetic disturbance effects on power systems. *IEEE Transactions on Power Delivery*, 8(3), 1993.

Kappenman J., Geomagnetic storms and their impacts on the US power grid, *Meta – R- 319 Report*, 2010.

Kappenman J., Geomagnetic storms and their impact on power systems, *IEEE Power Engineering review*, 1996.

Koen J., Gaunt T., Geomagnetically indced currents in the southern African electricity transmission network, *Proceedings of the IEEE Power Tech Conference*, Bologna, June 23-26, 2003.

Lahtinen M., and Elovaara J., GIC occurrences and GIC test for 400 kV System Transformer, *IEEE Transactions on Power Systems*, Vol. 17, No. 2, 555-561, 2002.

MATPOWER: Zimmerman R.D., Murillo-Sànchez, and Thomas R.J., MATPOWER: steady-state operations, planning and analysis tools for power system research and education, *IEEE Transactions on Power Systems*, Vol. 26, No. 1, 12-19, 2011.

Lu S., and Liu Y., A fundamental analysis of transformer GIC magnetization using the finite element approach, *Proceedings of the American Power Conference*, Illinois Inst. Technol., Illinois, USA, 1991.

Molinski T., Why utilities respect geomagnetically induced currents, *Journal of Atmospheric and solar and terrestrial Physics*, 64, 1765-1778, 2002.

NOAA, www.swpc.noaa.gov/communities/space-weather-enthusiasts last accessed on 25th October 2015.

NERC, GMDTF Interim Report: Effects of Geomagnetic disturbances on the Bulk power system, North American Electric Reliability Corporation, 2012.

Ngneugueu T., Marketos F., Devaux F., Bardsley R., Xu T., Barker S., Baldauf J., and Oliveira J., Behaviour of transformers under DC/GIC excitation: phenomenon, impact on design/design evaluation process and modelling aspect in support of design, *Proceedings of CIGRE*, Paris, August 26-31, 2012.

Piccinelli R., and Krausmann E., Space weather and power grids – A vulnerability assessment, EUR 26914 EN, ISBN 978-92-79-43971-1, 2014.

Pirjola R., Properties of matrices included in the calculation of geomagnetically induced currents (GICs) in power systems and introduction of a test model for GIC computing algorithms, *Earth Planet Space*, 61, 263-272, 2009.

Pirjola R., Pulkkinen A., and Viljanen A., Studies of space weather effects on the Finnish natural gas pipeline and on the Finnish high-voltage power system, Adv. Space Res., 31(4), 795—805, 2003.

Pirjola R., Kauristie K. Lappalainen H. Viljanen A., and Pulkkinen A., Space weather risk, Space Weather, 3, S02A02, 2005.

Pirjola R., Fundamentals about the flow of geomagnetically induced currents in a power system applicable to estimating space weather risks and designing remedies, Journal of Atmosheric and Solar –terrestrial Physics 64, 1967 – 1972, 2002.

Pulkkinen A., Bernabeu E., Eichner J., Beggan C., and Thomson W.P., Generation of 100-year geomagnetically induced current scenarios, Space Weather, 10, 2012.

Pulkkinen A., Pirjola R., and Viljanen A., Statistic of extreme geomagnetically induced current events, Space Weather, Vol. 6, S07001, (2008).

SCB Statistic Sweden website http://www.scb.se last accessed 20th June 2015.

SEA Swedish Energy Agency website: http://www.energimyndigheten.se/ last accessed 20th June 2015.

SSB, Statistics Norway, https://www.ssb.no/en/energi-og-industri/statistikker/elektrisitetaar, last accessed 20th October 2015

Statistics Finland, http://www.stat.fi/index_en. Last accessed on 15th October 2015

Statkraft, http://www.statkraft.com/energy-sources/ last accessed 20th October 2015

Wallling R.A., and Khan A.H., Characteristics of transformer exciting current during geomagnetic disturbances, *IEEE Transactions on Power Delivery*, Vol.6, No.4, 1991.

Viljanen A., Pirjola R., Wik M., Adam A., Pracser E., Sakharov Y., and Katkalov J., Continental scale modelling of geomagnetically induced currents, *J. Space Weather Space Clim*., 2, A17, 2012.

Viljanen A., and Pirjola R., Geomagnetically induced currents in the Finnish high-voltage power system, *Surveys Geophys.*, vol. 15, pp. 383–408, 1994.

Wik M., Pirjola R., Lundstedt H., Viljanen A. and Pulkkinen A., Space weather events in July 1982 and October 2003 and the effects on geomagnetically induced currents on Swedish technical systems, *Annales Geophysicae*, vol. 27, 1775-1787, 2009.

Zhou Q., and Bialek J.W., Approximate model of European interconnected system as a benchmark system to study effects of cross border trades, *IEEE Power Systems Transactions*, Vol. 20, nr.2, 782-788, 2005.

European Commission
EUR 27571 EN – Joint Research Centre – Institute for the Protection and Security of the Citizen

Title: Space Weather Impact on the Scandinavian Interconnected Power Transmission System

Authors: Roberta Piccinelli, Elisabeth Krausmann

Luxembourg: Publications Office of the European Union

2015 – 43 pp. – 21.0 x 29.7 cm

EUR – Scientific and Technical Research series – ISSN 1831-9424

ISBN 978-92-79-53761-5
doi:10.2788/939973

LB-NA-27571-EN-N

JRC Mission

As the Commission's in-house science service, the Joint Research Centre's mission is to provide EU policies with independent, evidence-based scientific and technical support throughout the whole policy cycle.

Working in close cooperation with policy Directorates-General, the JRC addresses key societal challenges while stimulating innovation through developing new methods, tools and standards, and sharing its know-how with the Member States, the scientific community and international partners.

Serving society
Stimulating innovation
Supporting legislation

doi:10.2788/939973

ISBN 978-92-79-53761-5

Publications Office